

Journal of Materials Chemistry C

Accepted Manuscript



This is an *Accepted Manuscript*, which has been through the Royal Society of Chemistry peer review process and has been accepted for publication.

Accepted Manuscripts are published online shortly after acceptance, before technical editing, formatting and proof reading. Using this free service, authors can make their results available to the community, in citable form, before we publish the edited article. We will replace this *Accepted Manuscript* with the edited and formatted *Advance Article* as soon as it is available.

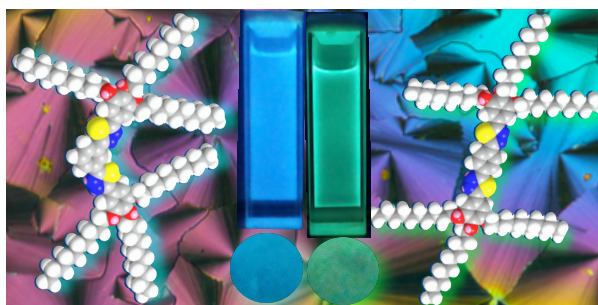
You can find more information about *Accepted Manuscripts* in the [Information for Authors](#).

Please note that technical editing may introduce minor changes to the text and/or graphics, which may alter content. The journal's standard [Terms & Conditions](#) and the [Ethical guidelines](#) still apply. In no event shall the Royal Society of Chemistry be held responsible for any errors or omissions in this *Accepted Manuscript* or any consequences arising from the use of any information it contains.

Dr. A. S. Achalkumar
Assistant Professor
Department of Chemistry
Indian Institute of Technology Guwahati
Guwahati – 781039, Assam, India
Phone: +91-361-258-2329
Fax: +91-361-258-2349
E-mail: achalkumar@iitg.ernet.in
achalkumar78@gmail.com



Table of Contents Graphic



Effect of Regioisomerism on the Self-assembly and Luminescence of Polycatenars

Effect of Regioisomerism on the Self-assembly and Photophysical Behavior of 1,3,4-Thiadiazole based Polycatenars

Suraj Kumar Pathak^a, Subrata Nath^a, Ravindra Kumar Gupta,^aD. S. Shankar Rao^b,
S. Krishna Prasad^b and Ammathnadu S. Achalkumar^{a,*}

^aDepartment of Chemistry, Indian Institute of Technology Guwahati, Guwahati, 781039, Assam, India ^bCentre for Nano and Soft Matter Sciences, Jalahalli, P. B. No. 1329, Bangalore, 560013, Karnataka, India.

Abstract: A new class of polycatenars where the central benzene ring is connected to two arms derived from substituted 1,3,4-thiadiazoles at 1,3- and 1,4-positions was synthesized and characterized. These thiadiazole based molecules are promising as they stabilize columnar phases over a wide range in comparison to their oxadiazole analogues. *para*-substituted polycatenars exhibited columnar hexagonal and/or columnar oblique phase, while *meta*-substituted polycatenars exhibited solely columnar oblique phase. *para*-Substituted polycatenars exhibit green emission, while the *meta*-substituted polycatenars exhibited blue emission in solution and film state. Stabilization of broad range columnar phase and luminescence in solid state make these new compounds promising from the view point of applications in emissive displays. The self-assembly and luminescence of these regioisomers was greatly influenced by the molecular structure.

Table of contents (TOC) Graphic



I. Introduction

Liquid crystal (LC) self-assembly of shape anisotropic molecules is a subject that is attracting a huge interest in recent years. This unique state of matter with a combination of the order and fluidity leads to special inherent properties that are important from the view points of basic and applied research.¹ Liquid crystals can be broadly classified as conventional and non-conventional, based on their shape.² Conventional LCs are comprised of two classes, that are calamitic (rod-like)³ or discotic (disc-like).⁴ Shape anisotropic molecules which stabilize mesophases, that are neither calamitic nor discotic fall under the class of non-conventional LCs.² Scientific curiosity in a quest to explore novel mesophases and applications, catapulted a flurry of activities in the design and syntheses of several different shape anisotropic molecules which deviate from the conventional rod or disc shapes.^{2, 5-12} Some

of the important examples of non-conventional systems are oligomers,⁵ bent-core molecules,⁶ polyhydroxy amphiphiles,^{7, 2c-e} octahedral complexes,⁸ star shaped molecules,⁹ rod-coil molecules,¹⁰ dendrimers¹¹ and polycatenars.¹²

Polycatenars or phasid-like LCs are one such class of non-conventional LCs comprising of central long aromatic rod connected to two terminal semi-discs with multiple flexible chains.^{12a-c} These molecules self-assemble into different LC phases due to the nanosegregation of aromatic units and flexible chains. Since polycatenars share the structural features of both calamitic and discotic LCs they exhibit various LC phases like nematic, smectic (lamellar), cubic, and columnar phases depending on the number of peripheral tails. Recently it was reported that some polycatenars based on indigoid system even exhibited mesophases similar to bent core LC phases.¹³ This synthetically flexible molecular motif can incorporate many functional moieties so as to develop multifunctional LCs. Incorporation of extended π -conjugated aromatic system in the polycatenar molecular structure is very important from the viewpoint of charge carrier and luminescence properties.¹⁴ Gin *et. al.* reported a polycatenar system with photophysical functions.^{12e} Yelamaggad *et. al.* incorporated hydrogen bonding oligopeptides in the polycatenar structure that stabilizes Columnar phase.¹⁵ Prasad *et.al.* introduced photoisomerizable azobenzene unit in the polycatenar structure.¹⁶ There are many reports on luminescent polycatenar LCs.^{14d-i}

Discovery of columnar self-assembly of discotics⁴ opened up a fascinating research area because of the various potential applications.¹⁸⁻²² This is because Col phases formed from discotics resemble molecular wires due to the one dimensional stacking of central rigid discs with an insulating sheath of peripheral tails, which help in one dimensional carrier migration.¹⁷ Columnar phase has the potential to realize many optoelectronic devices like photovoltaics,¹⁸ light emitting diodes,¹⁹ field effect transistors,²⁰ gas sensors²¹ and lubricants.²² Considering the synthetic difficulty and the rigidity for the structural tuning in DLCs, polycatenar LCs seems to be simpler alternative, as they can also stabilize Col phases.

Recently there is a renewed interest in the incorporation of heterocycles in the molecular design of mesogens due to the wide variety of structures and hence the resultant properties.²³ Hetero atoms like nitrogen, oxygen and sulfur provide a reduced molecular symmetry, strong lateral and/or longitudinal dipoles and a donor-acceptor interaction within the molecule, which in turn affects the LC self-assembly and electronic behavior of the mesogens.²³ Mesogens with heterocyclic moieties in their molecular structures, provide emission color tunability and also enable a polarized emission. This is an important property which finds application in the area of OLEDs.²⁴ Thus many polycatenar LCs bearing a heterocyclic moiety in their molecular structures are reported. There are relatively more reports on 1,3,4-Oxadiazole derivatives in comparison to their sulfur analogues 1,3,4-thiadiazole derivatives.^{26, 27}

1,3,4-Oxadiazole based molecules are known for their high luminescence efficiency, n-type behavior (electron transporting), resistance to oxidative degradation, hydrolytic and thermal stability. Hence they found application as n-type electroluminescent layers in organic light emitting diodes.^{23a-c, 25} Unfortunately, oxadiazole based mesogens have few drawbacks like high melting and clearing temperatures, narrow mesophase range and poor solubility which limits their applications.²⁶ Reports on their sulfur analogues, *i.e.* 1,3,4-thiadiazole based mesogens are limited in number. It is expected that, substitution of oxygen with sulfur increases the dipole moments, packing of molecules, viscosity, melting and clearing temperatures.^{23c, 27} In addition to this notion, partly the synthetic difficulty coupled with low yield curtailed the attempts in this direction. Calamitic LCs,²⁸ banana shaped LCs,²⁹ hydrogen bonded LCs,³⁰ and polymeric LCs³¹ based on 1,3,4-thiadiazole are reported. Very recently few polycatenar LCs^{26, 32} and star shaped mesogens^{33a} stabilizing columnar phase are reported. Our group reported the star shaped thiadiazole derivatives stabilizing hexagonal columnar mesophase.^{33b}

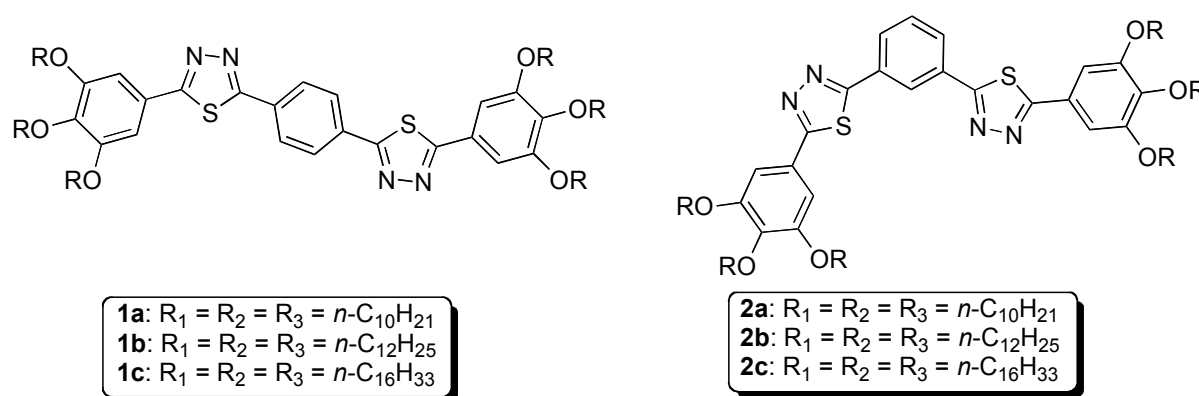


Figure 1. The molecular structures of compounds **1a-c** and **2a-c**.

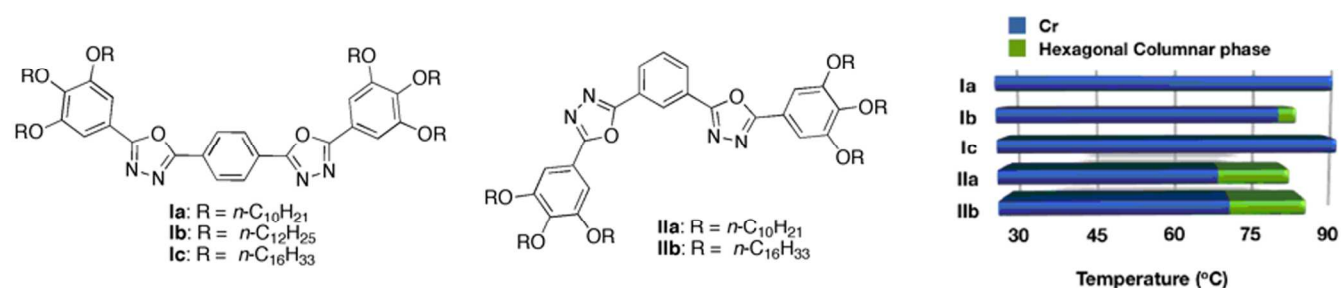
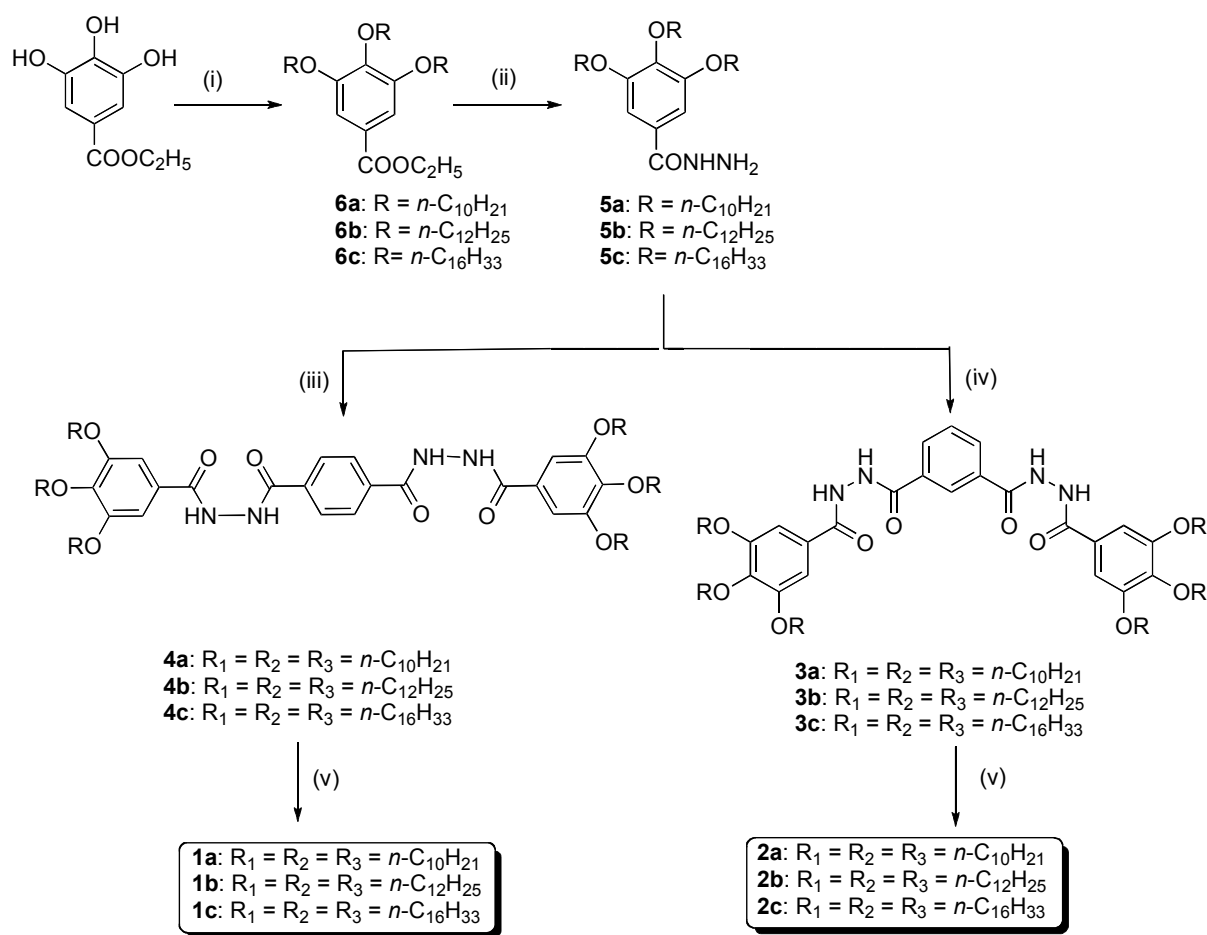


Figure 2. Polycatenars based on 1,3,4-oxadiazoles (**Ia-c**^{34b} and **IIa-b**^{34a}) that are comparable to 1,3,4-thiadiazole based polycatenars **1a-c** and **2a-c** of the present work; Bargraph showing the thermal behavior of compounds **Ia-c** and **IIa-b** (in heating cycle)

Scheme 1. Synthesis of 1,3,4-thiadiazole based liquid crystals



Scheme 1. Synthesis of 1,3,4-thiadiazole based polycatenars. Reagents and conditions: (i) *n*-bromoalkanes, anhydrous K₂CO₃, DMF, 80 °C, 24 h (70-90 %); (ii) NH₂NH₂·H₂O, *n*-butanol, reflux, 48 h (71-80 %); (iii) (a) 1,4-benzene dicarboxylic acid, SOCl₂, reflux, 6 h; (b) **5a-c**, THF, triethylamine, 12 h, reflux; (iv) (a) 1,3-benzene dicarboxylic acid, SOCl₂, reflux, 6 h; (b) **5a-c**, THF, triethylamine, 12 h, reflux; (v) Lawesson's reagent, toluene, reflux, 17 h (40-45 %).

As part of our efforts to combine luminescence with liquid crystalline order, we were interested to synthesize polycatenar liquid crystals, in particular hexacatenars based on 1,3,4-thiadiazole derivatives (Fig.1). We were also interested to compare their properties with the polycatenars based on 1,3,4-oxadiazole derivatives (Fig.2).³⁴ Additionally this also gives information on the effect of structure on the self-assembly process on going from hexacatenars to star shaped molecules. In this paper we report the synthesis of hexacatenars comprising five rings, among which two are 1,3,4-thiadiazoles. These two

thiadiazole rings are interconnected by a *para*- and *meta*-substituted benzene rings and having six-alkyl chains attached equally to two terminal benzene rings.

II. Results and discussion

II.1 Synthesis and molecular structural characterization (reference)

The synthetic strategy to prepare the hexacatenars is presented in scheme 1. Ethyl gallate was *O*-alkylated by heating with appropriate *n*-bromoalkanes in presence of anhydrous K₂CO₃ and anhydrous DMF. The synthetic methods of ethyl gallate and its alkoxy derivatives are reported prior.^{35a} These alkoxy esters (**6a-c**) were refluxed with hydrazine hydrate in *n*-butanol to obtain respective hydrazides (**5a-c**).^{33b, 34} Hydrazides **5a-c** were then coupled with terephthalic acid chloride to get 1,4-di-*N*-benzoylbenzohydrazides **4a-c**.³⁴ Similarly hydrazides **5a-c** on coupling with isophthalic acid chloride yielded 1,3-di-*N*-benzoylbenzohydrazides **3a-c**. Compounds **4a-c** and **3a-c** on refluxing with Lawesson's reagent^{35b} in toluene yielded polycatenars **1a-c** and **2a-c**.^{33b} Molecular structural characterizations were carried out using ¹H NMR, ¹³C NMR, IR spectroscopy and ESI-HRMS. (See the supporting information (SI) for the details).

II. 2. Thermal behavior

The liquid crystalline properties of these new hexacatenars belonging to two different series was investigated by polarizing optical microscopy (POM), thermogravimetric analysis (TGA), differential scanning calorimetry (DSC), and X-ray diffraction (XRD) studies. Liquid crystalline nature of polycatenar LCs was identified by the observation of strong birefringent and fluidic nature of the materials under POM. Further, the assignment of LC phase was made by correlating the typical textural pattern with the data obtained from XRD studies. The peak temperatures obtained in DSC traces due to phase transitions were found to be in accordance with POM observations. The transition temperatures, mesophase sequence and the corresponding enthalpy changes are summarized in table 1. The bargraph provided in Fig.3 accounts the thermal behavior of these compounds in first heating cycle. The thermal stability of the compounds were analysed by TGA showed that all the compounds were thermally stable upto ≈ 250 °C and complete degradation occurred at around 600 °C. (See the SI).

In the following sections, we discuss the LC behavior of the thiadiazole based polycatenars using the above-mentioned complementary techniques. From the bargraph shown in Fig. 3, it is evident that in the case of *p*-substituted polycatenars melting temperature decreases with the increase in chain length, while decrease in clearing point is not regular. The mesophase range is wider for compound **1b**

with medium chain length, while it is short for compound **1c** with highest chain length. In the case of *m*-substituted polycatenars, there is no such trend in the variation of melting points with respect to chain length, but show a constant decrease in the clearing point. Again as in the case of *p*-substituted polycatenars, compound **2b** with medium chain length shows a wide range of mesophase, while compound **2c** shows the shortest mesophase width. Thus from these information we can infer that for

Table 1. Phase transition temperatures ^a (°C) and corresponding enthalpies (kJ/mol) of DLCs

Compound	Phase sequence	
	Heating	Cooling
1a	Cr ₁ 45.3 (10.3) Cr ₂ 51.5 (120.7) Cr ₃ 79.5 (266.5) Col _h 95.9 (11.3) I Cr ₁ 34.8 (205.3) ^c Cr ₂ 78.3 (358.1) Col _h 95.9 (20.2) I	I 94.6 (11.3) Col _h 28.4 (13.7) Cr I 94.6 (20.2) Col _h 28.5 (24.8) Cr
1b	Cr ₁ 55.6 (76.5) Cr ₂ 67.6 (14.8) Cr ₃ 78.1 (131) Col _{ob} 98.9 (7.1) I Cr ₁ 53 (269) ^c Cr ₂ 76.4 (365) Col _{ob} 98.4 (15.7) I	I 97.3 (7.2) Col _{ob} 44 (19.1) Cr I 97.3 (16.4) Col _{ob} 44 (45.4) Cr
1c	Cr 70.2 (202.5) Col _h 83.5 (1.5) I Cr ₁ 55.5 (502) Cr ₂ 63.99 (78.1) Cr ₃ 73.2 (6.2) Col _h 81.7 (17) I	I 80.4 (5.3) Col _h 51 Col _{ob} ^b 46.1 (142.3) Cr I 80.6 (17.6) Col _h 51 Col _{ob} ^b 46.1 (262) Cr
2a	Cr ₁ 42.2 (10.6) Cr ₂ 62 (22.5) Col _{ob} 97.9 (12.6) I Cr ₁ 25.03 (62.2) Cr ₂ 62 (49) Col _{ob} 97.8 (20.2) I	I 96.9 (11.5) Col _{ob} 53.4 (25) Cr ₂ 19.7 (29.9) Cr ₁ I 96.9 (20.1) Col _{ob} 53.51 (45.2) Cr ₂ 19.8 (54.5) Cr ₁
2b	Cr 57.2 (135.7) Col _{ob} 94.4 (11.7) I Cr ₁ 48.4 (97.7) Cr ₂ 55.8 (103.3) Cr ₃ 59.9 (24.8) Col _{ob} 94.3 (25) I	I 93.4 (10.8) Col _{ob} 54.9 (20.4) Cr ₁ 41.8 (71.7) Cr ₂ I 93.4 (24.6) Col _{ob} 54.9 (48.6) Cr ₂ 41.8 (161.9) Cr ₁
2c	Cr ₁ 75.6 (147.3) Col _{ob} 87 (8) I Cr ₁ 75.7 (499.6) Col _{ob} 87 (27) I	I 86 (8.2) Col _{ob} 64.6 (151.7) Cr I 86 (28.4) Col _{ob} 64.5 (516.5) Cr

^a Peak temperatures in the DSC thermograms obtained during the first and second heating-cooling cycles at 5 °C/min. ^b The phase observed is monotropic. Col_h = Columnar hexagonal phase; Col_{ob} = Columnar oblique phase. ^c exothermic crystallization.

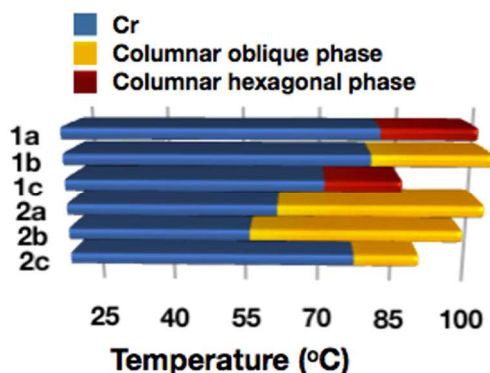


Figure 3. Bargraph summarizing the thermal behavior of compounds **1a-c** and **2a-c** (heating cycle)

this class of polycatenars, the appropriate length of peripheral chains is an important factor in deciding the mesophase width. In cooling cycle, both the series of compounds showed a common trend, *i.e.* a constant decrease in the mesophase width with the increase in chain length.

Thiadiazole based *p*-substituted polycatenar molecule **1a** with shortest chain, exhibited enantiotropic columnar mesophase spanning a thermal range of 16 degrees in heating cycle after passing through two Cr-Cr transitions at ≈ 45 °C and 52 °C with an enthalpy change of 10.3 kJ/mol and 120.7 kJ/mol respectively as evidenced by DSC thermograms. Further heating shows that around 80 °C, a transition to birefringent fluidic liquid crystalline phase was observed, which stays upto 96 °C before passing to an isotropic liquid. On cooling from isotropic liquid state small spherulites developed from the homeotropic dark field of view (Fig. 4a and b), persisted till 28 °C. The compound crystallizes below this temperature (Fig. 4c).

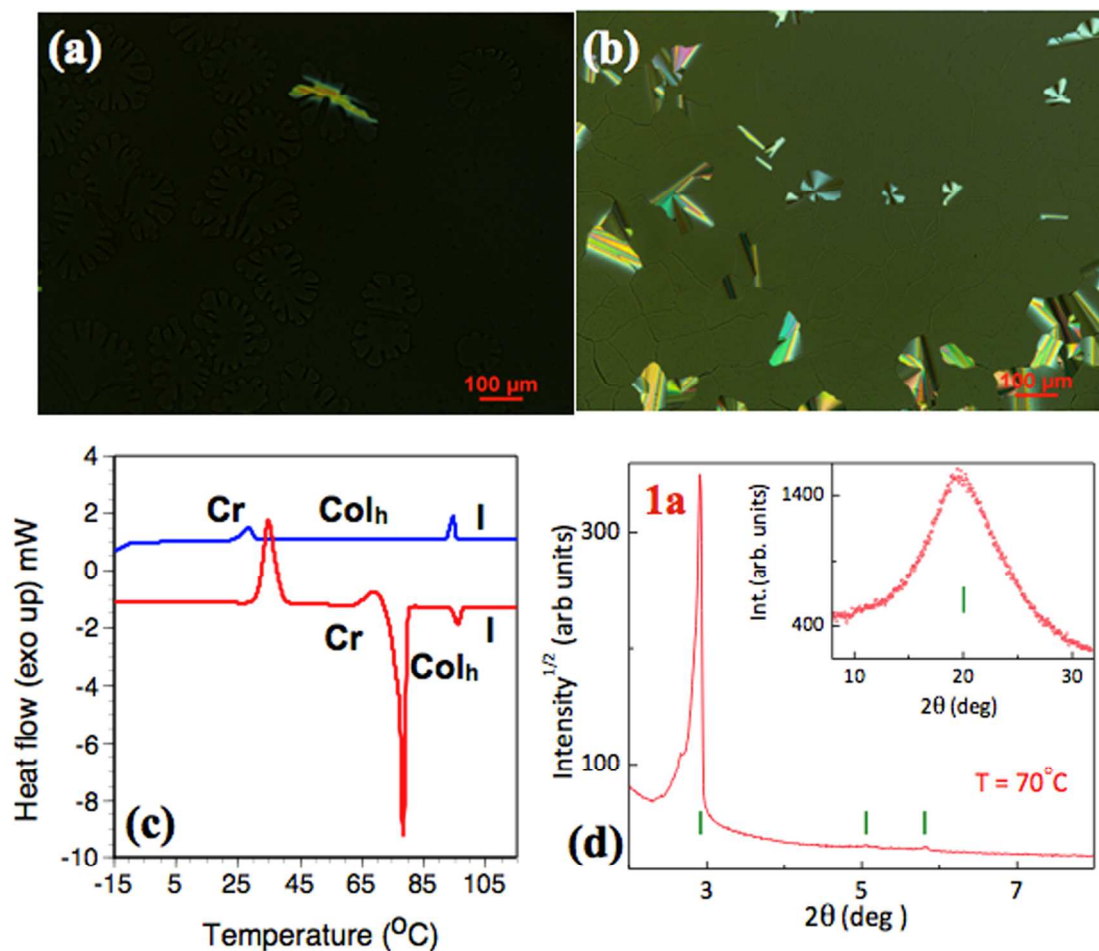


Figure 4. Photomicrographs of textures as seen by POM for the Col_h phase of compound **1a** (a) at 90 °C; (b) at 70 °C; DSC traces obtained for first cooling (blue trace) and second heating (red trace) cycles of compound **1a** at a rate of 5 °C/min. (c); XRD profiles depicting the intensity against the 2θ obtained for the Col_h phase of compound **1a** at 70 °C (d)

Powder X-ray diffraction studies on compound **1a** at different temperatures was done to determine the symmetry of the enantiotropic columnar mesophase. The results of indexing the reflections of the XRD profiles are tabulated in table 2. The X-ray profile of compound **1a** at 90 °C showed three reflections at small angle region corresponding to the d -spacings 29.94 Å, 17.27 Å and 15 Å that can be indexed into Miller indices 100, 110 and 200 respectively (SI). In the wide angle region a relatively diffused peak

Table 2. Results of (hkl) indexation of XRD profiles of the compounds at a given temperature (T) of mesophases^a

Compounds ($D/\text{Å}$)	Phase (T/°C)	d_{obs} (Å)	d_{cal} (Å)	Miller indices (hkl)
1a (48.3)	Col _h (90)	29.94 17.27 15.00 4.47 (h_a)	29.95 17.29 14.97	100 110 200
	Col _h (70)	30.30 17.49 15.21 4.43 (h_a)	30.31 17.50 15.16	100 110 020
1b (53.3)	Col _{ob} (90)	34.23 33.39 32.21 4.49 (h_a)	34.23 33.39 32.21	010 100 110
1c (63.4)	Col _h (70)	35.88 20.75 4.51 (h_a)	35.90 20.73	100 110
	Col _{ob} (50)	40.00 37.81 21.89 18.71 13.92 10.42 7.51 6.07 4.20 (h_a) 4.19 (h_c)	40.00 37.81 21.89 18.91 14.02 10.40 7.56 6.17	010 110 -110 220 -210 420 550 -430

^aThe average diameter (D) of the polycatenars (estimated from Chem 3D Pro 8.0 molecular model software from Cambridge Soft). d_{obs} : spacing observed; d_{cal} : spacing calculated (deduced from the lattice parameters; a for Col_h phase; a and b for Col_{ob} phase; γ is the column tilt angle). The spacings marked h_a and h_c correspond to diffuse reflections in the wide-angle region arising from correlations between the alkyl chains and core regions, respectively.

corresponding to the d spacing of 4.47 Å was observed. The first three reflections follow the reciprocal spacing ratio of 1:0.58:0.5 of a hexagonal lattice. The diffuse peak at the wide angle corresponds to the packing of flexible alkyl tails in the columnar phase. The peak corresponding to the stacking of cores

was not observed showing that the intermolecular interactions are not that strong. The hexagonal lattice parameter ' a ' calculated was found to be 34.58 Å, while the lattice area and molecular volume was found to be 1035.04 Å², and 4627.7 Å³ respectively. From these values, the number of molecules present in an unit cell was derived and found to be 2.09. This can be explained as below. In principle we can consider both dumbbell-like and hemidisc-like conformations of *p*-substituted polycatenar **1a** formed due to the different orientations of two thiadiazole rings (Fig.5). Among these conformations dumbbell-like conformer (Fig. 5a) is somewhat staright, while hemidisc-like conformer (Fig. 5b) is little bent and all alkyl chains are towards one side. In spite of these conformations, these molecules do not differ much

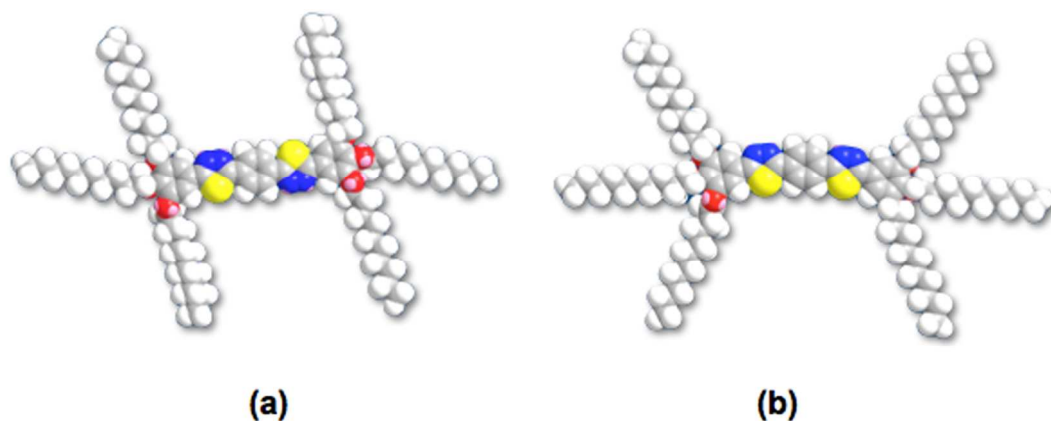


Figure 5. Molecular models showing 'dumbbell-like' conformation (a) and hemidisc-like conformation (b) for compound **1a**.

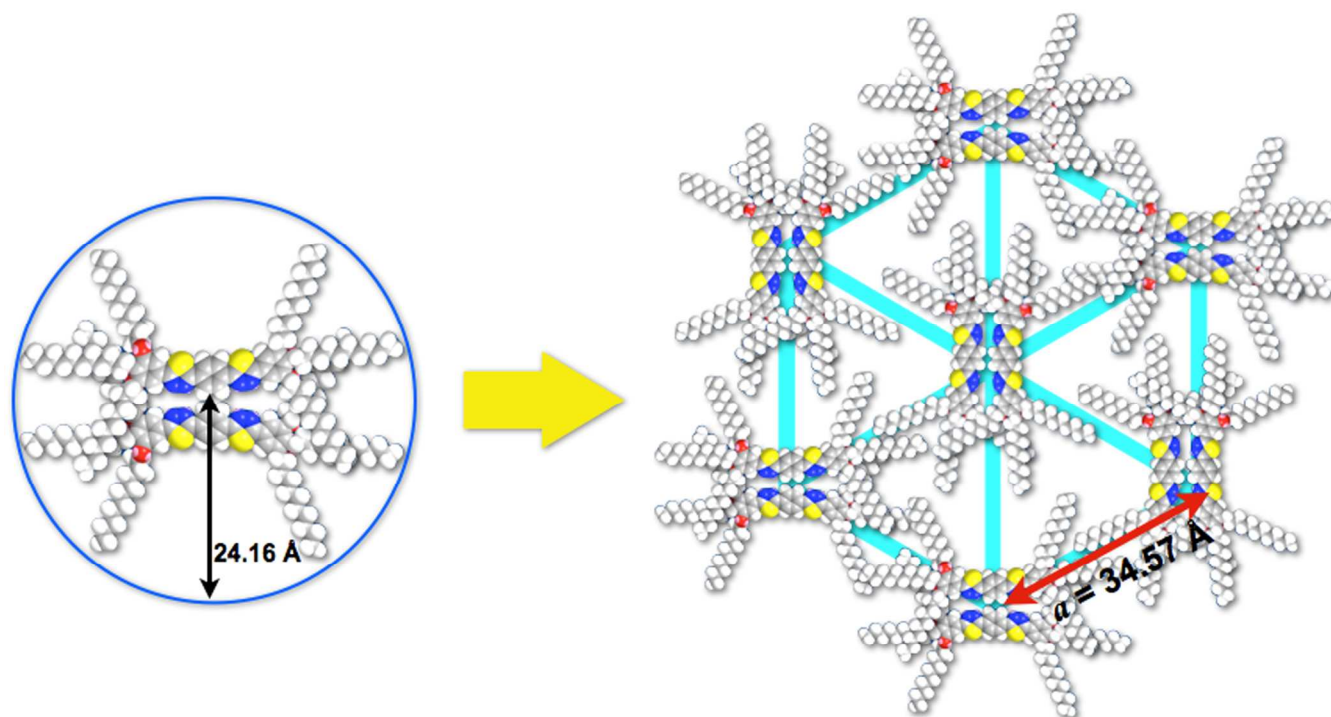


Figure 6. Schematic showing the self-organization of hexacatenar **1a** into hexagonal columnar (Col_h) lattice with inter-digitation of alkyl tails. Space filling energy minimized (all-*trans*) molecular model of **1a** derived from molecular mechanics (MM2) method.

in their molecular diameter as obtained from the molecular models (Table 2). This is because of the larger atomic size of sulfur which leads to a larger bending angle. From the XRD studies, it is evident that a columnar slice of thickness of 4.47 Å consists of two molecules.

Thus among the two conformations, it is reasonable to assume that two hemidisc shaped conformers (Fig. 5b) can pack side by side to form a disc with efficient space filling. Further the voids were filled by the flexible chains (interdigitation) of polycatenars from the adjacent columns or by chain folding. Eventhough the discs formed by these polycatenars look slight elliptical in shape, their time and space averaging results in a circular shape (Fig. 6). Similar packing arrangement is reported for analogous oxadiazole based polycatenars.^{34b} These discs in turn self-assemble to form a columnar phase with hexagonal symmetry (Fig. 6). The hexagonal cell parameter 'a' obtained from XRD studies was found to be 30% less than the molecular diameter calculated from Chem 3D Pro 8.0 software. This points to the interdigitation or folding of alkyl tails of polycatenars in adjacent columns. X-ray diffraction carried out at lower temperature (70 °C) also showed the similar pattern with a slight increase in the lattice parameter 'a' (Fig. 4d and table 2).

Compound **1b** also showed slightly higher isotropic temperature than compound **1a**, which on cooling from the isotropic melt showed the formation of Columnar phase with the appearance of a mosaic texture (Fig. 7a). At some regions spherulitic texture was also seen (Fig. 7b). Both of these textures in some cases reported for Col_h phase but mosaic texture is often seen for Col_r phase.^{36, 37} Even Columnar oblique phase (Col_{ob}) also sometime show fan shaped textures.^{35a} Since there are minor differences in the structures of these different columnar phases, assignment of the symmetry of the mesophase exclusively based on textures is often misleading.

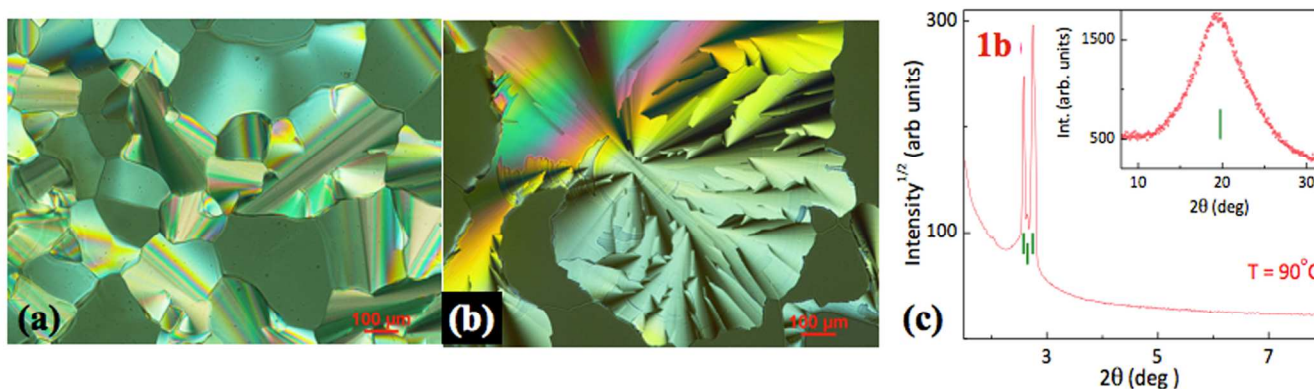


Figure 7. Photomicrographs of textures as seen by POM for the Col_{ob} phase of compound **1b** (a) at 90 °C; (b) at 65 °C; XRD profiles depicting the intensity against the 2θ obtained for the Col_{ob} phase of compound **1b** at 90 °C (c)

The diffraction pattern obtained from the powder XRD studies of the unaligned sample cooled from isotropic liquid state at 90 °C is explained below. Indexing of one-dimensional (1D) intensity vs 2θ profile deduced from the powder 2D pattern at 90 °C shows three strong reflections at low angle region ($0 < 2\theta < 5^\circ$) with the respective spacing ratio of 1: 0.97: 0.94, which could be assigned to (010), (100) and (110) reflections from a Col_{ob} lattice (Fig. 7c). This belongs to a primitive planar space group P_1 and hence there are no reflection conditions as in the case of Col_h or Col_r . In the wide angle region, a broad diffused peak corresponding to the packing of flexible alkyl tails was noticed at a d spacing of 4.49 Å. The oblique lattice had the cell parameters $a = 37.38$ Å and $b = 38.31$ Å with the angle between the two dimensional (2D) lattice directions, *i.e.* $\gamma = 26.7^\circ$. Thus the shape of the 2D lattice is a parallelogram.

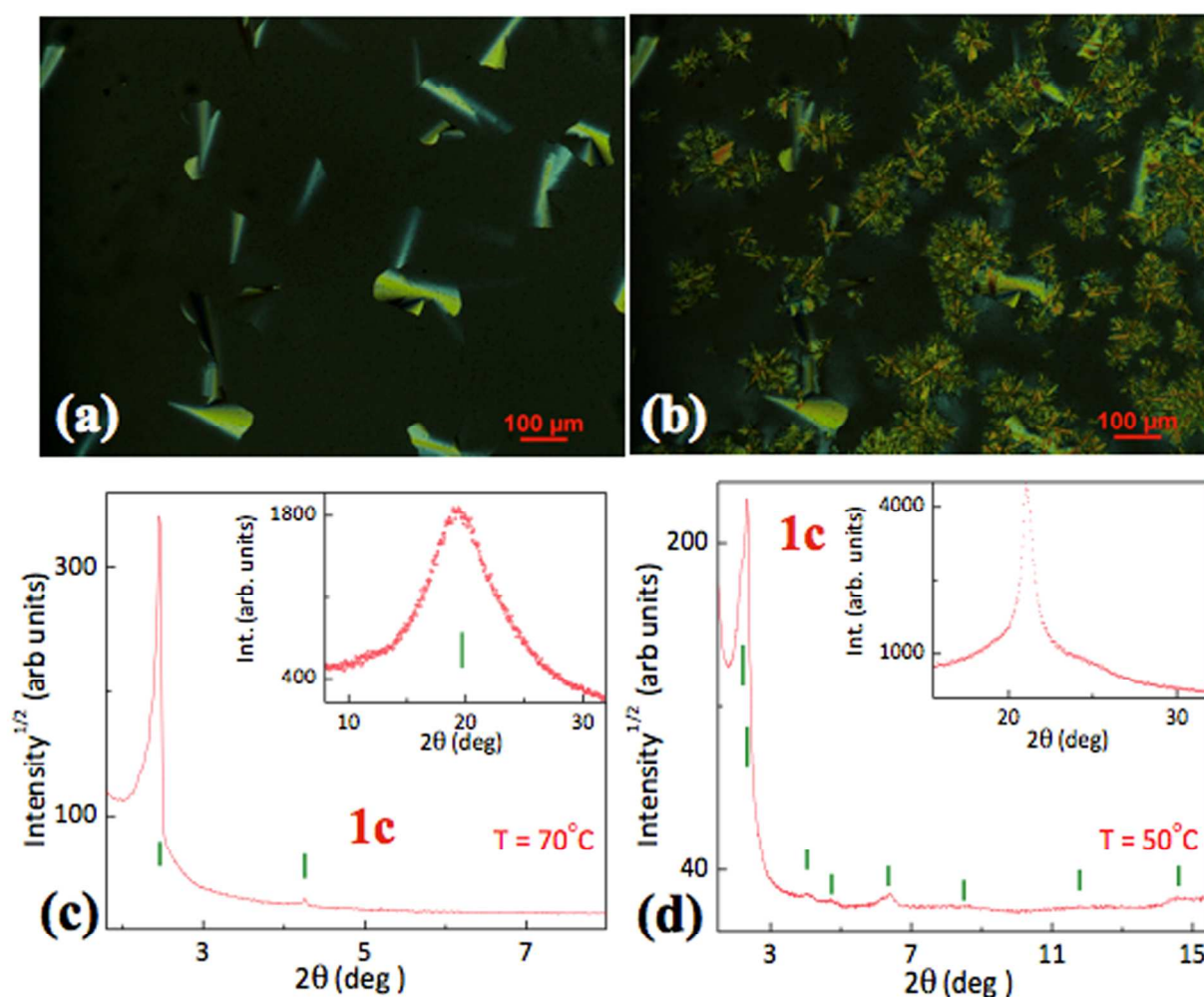


Figure 8. Photomicrographs of textures as seen by POM for the Col_h phase of compound **1c** (a) at 70 °C; (b) Col_{ob} phase at 50 °C; XRD profiles depicting the intensity against the 2θ obtained for the Col_h phase of compound **1c** at 70 °C (c) and Col_{ob} phase at 50 °C

Polycatenar molecule **1c** with longest chains in this series showed a reduced mesophase range of around 13 degrees in heating cycle with an isotropic temperature of 84 °C. Crystal to mesophase transition observed as a broad peak in DSC thermogram with an enthalpy change of 202.5 kJ/mol. In the cooling cycle Col_h phase appeared with a characteristic texture of large homeotropic regions with some bright defects interspersed (Fig. 8a). This was also corroborated by XRD studies carried out at 70 °C, with a characteristic pattern commonly observed for Col_h phase. Around 51 °C the small needles grow over the mosaic pattern and covers the entire area (Fig. 8b). Such needle like textures are reported for Col_r phase.³⁷ XRD studies carried out at 50 °C, showed several peaks from low angle to mid angle region ($0 < 2\theta < 15^\circ$), in addition to two diffused peaks at wide angle region. The *d* spacings obtained for these reflections are corresponding to the Miller indices (010), (110), (-110), (220), (-210), (420), (550) and (-430). Lattice parameters derived from these reflections were found to be $a = 41.68 \text{ \AA}$ and $b = 46.21 \text{ \AA}$ with the angle between them $\gamma = 30.04^\circ$. Since the value of $\gamma \neq 90^\circ$, we can conclude that the phase under investigation is Col_{ob}.

It is interesting to note that all the three molecules showed different thermal behavior, *i.e.* compound **1a** showed Col_h phase exclusively, compound **1b** showed only Col_{ob} phase, while compound **1c** showed both the columnar phases, even though Col_{ob} phase observed was a monotropic phase. Except the chain length, there is no other modification, thus the chain length is an important factor in deciding the symmetry of Col phase observed here. In the case of discotics with the increase in peripheral chain length, it is usual to predict a cross over from rectangular to hexagonal columnar phase.^{36,38} But such tendency is not seen in this class of polycatenars. It is to be noted that corresponding oxadiazole based polycatenars exhibited either crystalline or Col_h phase, and the mesophase stabilization is limited to certain chain length. In the case of present series of thiadiazoles all the compounds were liquid crystalline and the medium chain length compound **1b** exhibited broad mesophase range in heating cycle. In the cooling cycle a different trend was observed, *i.e.*, with the increase in chain length a decrease in the mesophase width was observed. Oxygen to sulphur substitution in the molecular structure definitely improved the mesophase width of these compounds with respect to their oxadiazole counterparts.^{34b}

Thiadiazole based *m*-substituted polycatenar **2a** on heating showed Cr-Cr transition at $\approx 42^\circ\text{C}$ before passing to a birefringent fluidic mesophase at 62°C . This compound on further heating showed a mesophase to isotropic state transition at $\approx 98^\circ\text{C}$ with an enthalpy change of 13 kJ/mol. On cooling from the isotropic melt, large pseudofocal fan shaped texture with spherulitic domains developed with

the concurrent occurrence of homeotropic domains (Fig. 9a). This on further cooling remains unchanged except a change in color and loss of fluidity; eventhough a mesophase to crystal transition with an enthalpy change of 25 kJ/mol at ≈ 54 °C was observed in DSC (Fig. 9b). Powder XRD studies carried out at 90 °C and 70 °C (Fig.9c) showed that the phase under investigation is Col_{ob} phase (Table 3). XRD studies at 90 °C, showed three relatively sharp peaks at low angle followed by two diffused peaks at wide angle. The first three reflections with d spacings of 32.41 Å, 31.03 Å and 15.52 Å, were corresponding to Miller indices (010), (110) and (-110) respectively. These d spacings were in the ratio of 1: 0.96: 0.48, with lattice parameters a and b found to be 31.52 Å and 41.39 Å respectively with $\gamma = 38.47$ Å. The first diffused peak observed with a d spacing of 4.57 Å corresponds to the packing of flexible alkyl tails, while the second peak with a d spacing of 3.77 Å corresponds to the core-core distance. The number of molecules present in a unit cell was found to be 2.2. The XRD studies carried out at 70 °C also showed a similar pattern as shown in figure 9c.

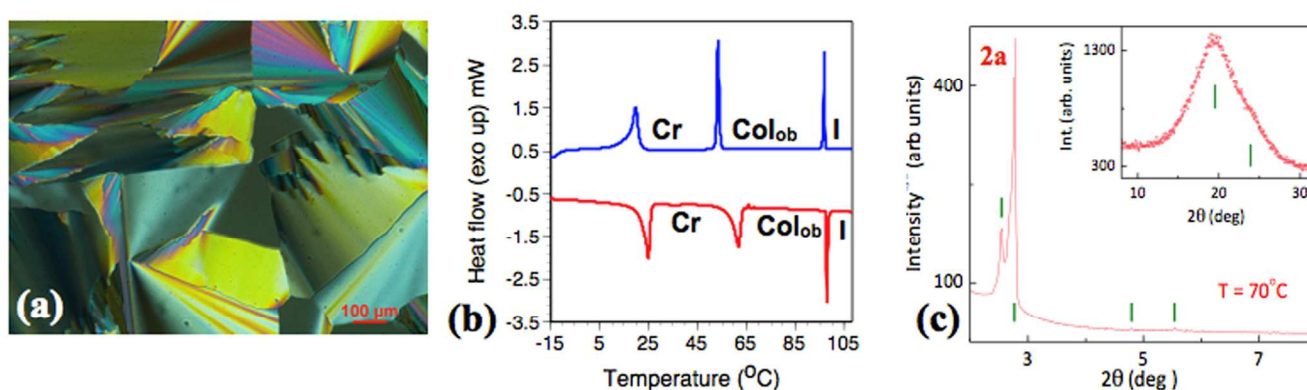


Figure 9. Photomicrograph of texture as seen by POM for the Col_r phase of compound **2a** at 70 °C (a); DSC traces obtained for first cooling (blue trace) and second heating (red trace) cycles of compound **2a** at a rate of 5 °C/min (b); XRD profiles depicting the intensity against the 2θ obtained for the Col_h phase of compound **2a** at 70 °C (c).

The packing of two molecules in a columnar slice can be described as below. The m -substituted polycatenar **2a** can exist in two possible conformations as shown in figure 10. As the XRD data suggests that on an average two molecules must be packed inside the unit cell, then they must arrange side by side to ensure the space filling. These sets of two molecules forming a disc, later self-assemble to form columns, and these columns in turn self-organize to form a 2D lattice of parallelogram.

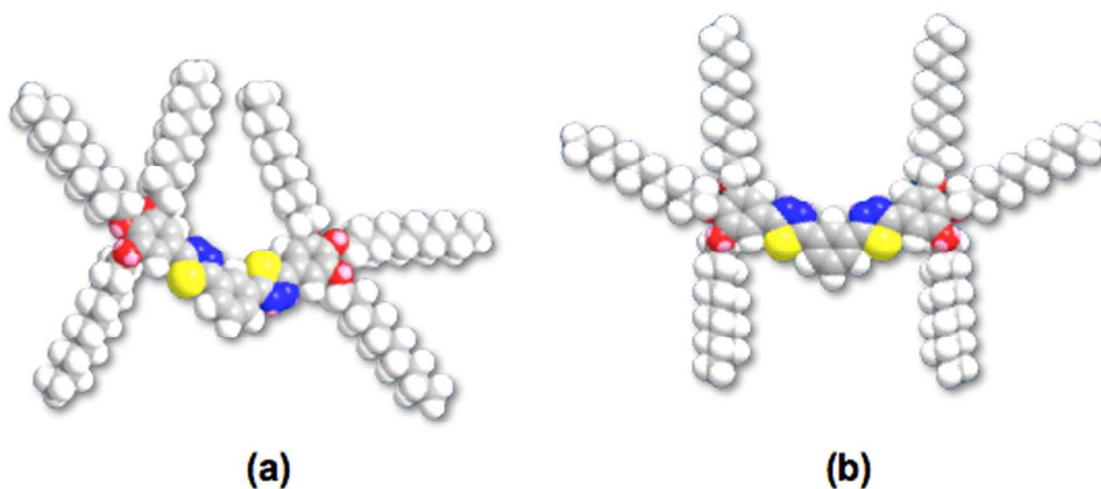


Figure 10. Molecular models obtained from Chem 3D showing the possible molecular conformations of compound **2a**.

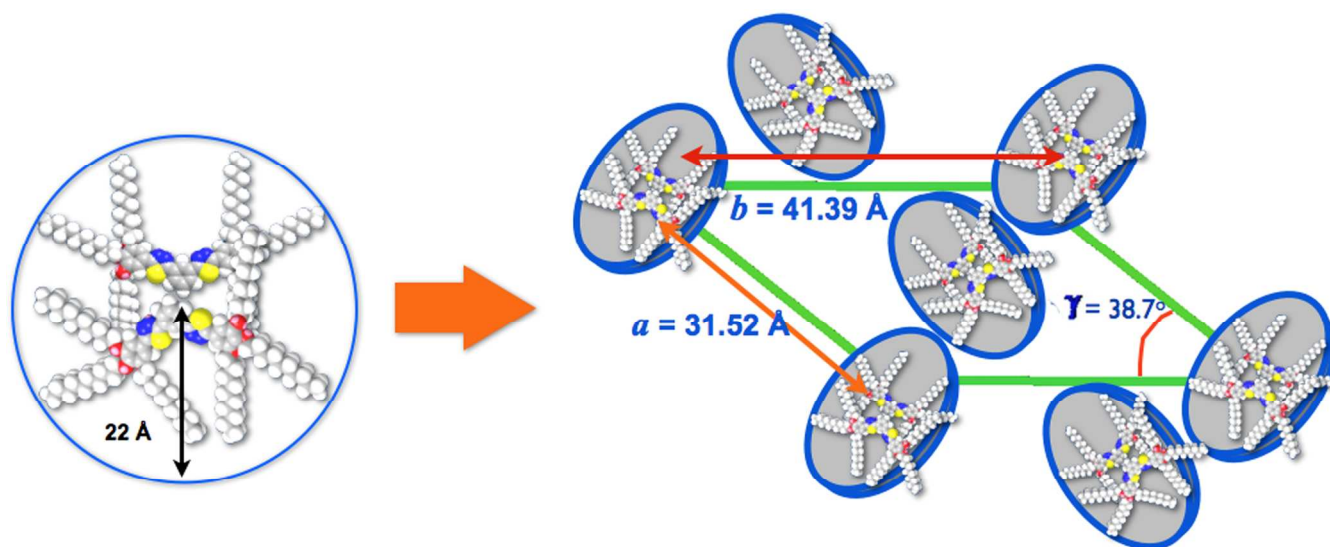


Figure 11. Schematic showing the self-organization of hexacatenar **2a** into columnar oblique (Col_{ob}) lattice. Space filling energy minimized (*all-trans*) molecular model of **2a** was derived from molecular mechanics (MM2) method. Ellipses denote tilted discs with respect to columnar axis.

Polycatenars **2b** and **2c** showed enantiotropic monomesomorphic behavior. Pseudofocal conic fan shaped texture observed for both of these compounds (Fig. 12). Powder XRD investigations suggested that these compounds stabilize Col_{ob} phase (Table 3).

In the first series of *p*-substituted polycatenars the reduction in isotropic temperature is not regular in heating cycle, while in the second series of *m*-substituted polycatenars there is a gradual reduction in the isotropic temperature with the increase in chain length (Fig. 3). Both the series of

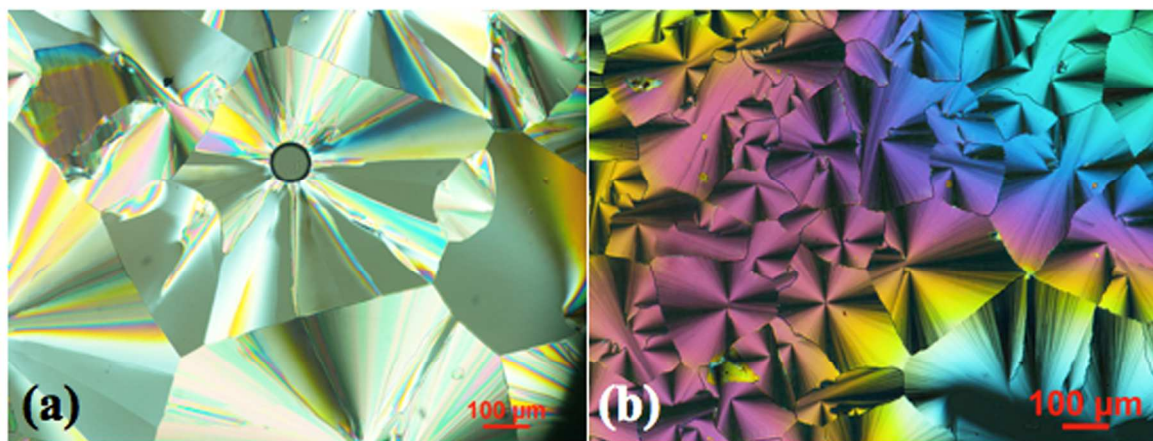


Figure 12. Photomicrograph of texture as seen by POM for the Col_{ob} phase of compound **2b** at 80 °C (a); and for compound **2c** at 84 °C (b)

Table 3. Results of (*hkl*) indexation of XRD profiles of the compounds at a given temperature (*T*) of mesophases^a

Compounds (<i>D</i> /Å)	Phase (<i>T</i> /°C)	<i>d</i> _{obs} (Å)	<i>d</i> _{cal} (Å)	Miller indices <i>hkl</i>
2a 44.01	Col _{ob} (90)	32.41 31.03 15.52 4.57 (<i>h_a</i>) 3.77 (<i>h_c</i>)	32.41 31.03 15.52	010 110 -110 001
	Col _{ob} (70)	34.74 31.90 18.42 15.96 4.54 (<i>h_a</i>) 3.72 (<i>h_c</i>)	34.74 31.90 18.42 15.95	010 110 -110 020 001
2b 48.5	Col _{ob} (80)	36.10 34.82 33.55 4.55 (<i>h_a</i>) 3.71 (<i>h_c</i>)	36.10 34.82 33.55	010 110 100 001
2c 58.8	Col _{ob} (82)	40.98 38.40 37.03 21.38 4.59 (<i>h_a</i>) 3.75 (<i>h_c</i>)	40.98 38.40 37.03 21.23	010 100 110 210 001

^aThe diameter (*D*) of the polycatenar (estimated from Chem 3D Pro 8.0 molecular model software from Cambridge Soft). *d*_{obs}: spacing observed; *d*_{cal}: spacing calculated (deduced from the lattice parameters; *a* for Col_h phase; *a* and *b* for Col_{ob} phase; γ is the column tilt angle). The spacings marked *h_a* and *h_c* correspond to diffuse reflections in the wide-angle region arising from correlations between the alkyl chains and core regions, respectively.

molecules showed reduction in the thermal range with the increase in chain length. When compared to *p*-substituted polycatenars **1a-c**, which exhibited Col_h and/or Col_{ob} phase, *m*-substituted polycatenars **2a-c** showed broader mesophase range and stabilized Col_{ob} phase exclusively. We need to recall here that among the *p*-substituted polycatenars from first series, the peak corresponding to core-core stacking was absent. On the contrary all the *m*-substituted polycatenars show the reflection corresponding to core-core stacking suggesting that, there is an enhanced core-core interaction in this series of compounds. It is understandable that for the stabilization of Col_{ob} phase, enhanced core-core interactions are essential because the tilt of the cores in one column must be related to the tilt of cores in another column in certain way.³⁶

Mesomorphic behavior of thiadiazole-based polycatenars **1a-c**, **2a** and **2c** of the present work can be compared to their oxadiazole counterparts **Ia-c**^{34b} and **IIa-b**^{34a}, which are reported earlier (Fig. 2). On comparing thermal behavior it is evident that thiadiazole-based *p*-substituted polycatenars stabilize Col_h and/or Col_{ob} phase, while their oxadiazole counterparts **Ia-c**^{34b} stabilized crystal/ Col_h phase. It is to be noted that analogous *m*-substituted polycatenars based on 1,3,4-oxdiazoles exhibited Col_h phase exclusively, irrespective of the chain length (Fig. 2).^{34a} This also supports the enhanced core-core interactions in the case of these thiadiazole based *m*-substituted polycatenars. Hetero atom sulphur in the molecular structure is another contributing factor due to the attractive S...S interactions, which is a well-known fact in the case of chalcogen based semiconductors.³

Mesophase width was increased in the case of thiadiazole derivatives in comparison to their oxadiazole analogues. This behavior is in line with the behavior of star shaped 1,3,4-thiadiazole derivatives recently reported, where star shaped 1,3,4-thiadiazoles exhibited wide range enantiotropic Col_h phase in comparison to their oxadiazole counterparts.^{33b} Thus thiadiazole moiety enhances the mesogenic behavior due to favorable interactions. Polycatenar thiadiazoles exhibited reduced mesophase range when compared to the star shaped thiadiazole derivatives.

III. Photophysical properties

Photophysical properties of the polycatenars **1a-c** and **2a-c** in solution are depicted in table 4. It is expected that due to the difference in substitution pattern between the two series, there must be a considerable difference in the photophysical properties. Absorption and fluorescence spectra of the compounds **1a-c** and **2a-c** were taken in THF (Fig. 13).

As can be seen, the absorption spectra for the solutions of *p*-substituted polycatenars **1a-c** showed single absorption maxima in a range of 360-365 nm. The absorption maxima of *m*-substituted polycatenars **2a-c** compounds exhibited a hypsochromic shift with an absorption maxima centered at around 335-337 nm. Large values of molar extinction coefficients showed that these are highly delocalized electronic systems ($\epsilon = >18,650 \text{ M}^{-1} \text{ cm}^{-1}$). Based on the similarity to reported 1,3,4-oxadiazole and thiadiazole based systems,^{33b} the single absorption band of these systems is attributed to π - π^* transition of the aromatic system. Optical bandgaps of these systems were calculated from the absorption onset values. Compounds **1a-c** showed a band gap of 3 eV, while compounds **2a-c** showed a slightly higher bandgap of 3.23 eV. This shows that π electron cloud is delocalized to a higher extent in the case of *p*-substituted compounds (**1a-c**) in comparison to *m*-substituted compounds (**2a-c**). Compared to their star shaped analogue *i.e.* 1,3,5-benzene trisubstituted thiadiazole derivative (optical band gap of 3.1 eV) with nine decyloxy chains, compounds **1a-c** showed a bathochromic shift of 20 nm in the absorption maximum, while **2a-c** showed a hypsochromic shift of 10 nm. When compared to the corresponding oxadiazole derivatives *p*- and *m*-substituted thiadiazole derivatives, showed a red shift of 26 nm.³⁴

Emission spectra of compounds **1a-c** exhibited a single emission maximum centered around 480-483 nm with large Stoke's shift of 115-121 nm. Compounds **2a-c** showed emission with their maxima centered around 446-450 nm, with a Stoke's shift of 111-114 nm. As can be seen from the table, there was no much difference in the absorption and emission properties with respect to chain length.^{33b, 34, 37} When compared to their star shaped analogue with nine decyloxy chains, compounds **1a-c** showed a bathochromic shift of 9 nm in the emission maximum, while **2a-c** showed a hypsochromic shift of 24 nm. As can be seen in the Fig.13, green light was observed in the emissive state for compounds **1a-c**, while blue light was observed for compounds **2a-c** on irradiation with the UV light of 365 nm wavelength. When compared to the corresponding oxadiazole derivatives *p*-substituted thiadiazole derivatives showed a red shift of 15 nm, while *m*-substituted thiadiazole derivatives, showed

a red shift of 21 nm.³⁴ As a representative case we measured the relative quantum yield for compounds **1a** and **2a** with respect to quinine sulphate solution (0.1 M H₂SO₄ with a quantum yield of 0.54). Compound **1a** showed a relative quantum yield of 0.4, while compound **2a** with a slightly lesser value (0.35) (see SI). These compounds showed slightly higher quantum yield with respect to their star shaped analogue **III** (0.31).^{33b}

Table 4. Photophysical properties of polycatenars^a

Entry	Absorption (nm)	Emission ^b (nm)	Stokes shift nm (cm ⁻¹)	λ_{onset} (nm)	$\Delta E_{\text{g, opt}}^{\text{c,d}}$
1a	365	480	115 (6564)	414	3.0
1b	360	483	118 (7075)	414	3.0
1c	360	481	121 (6987)	412	3.02
2a	335	446	111 (7429)	383	3.24
2b	336	450	114 (7540)	385	3.23
2c	337	449	112 (7402)	385	3.23

^amicromolar solutions in THF; ^b excited at the respective absorption maxima; ^c Band gap determined from the red edge of the longest wavelength (λ_{onset}) in the UV-vis absorption spectra; ^d In volts (V)

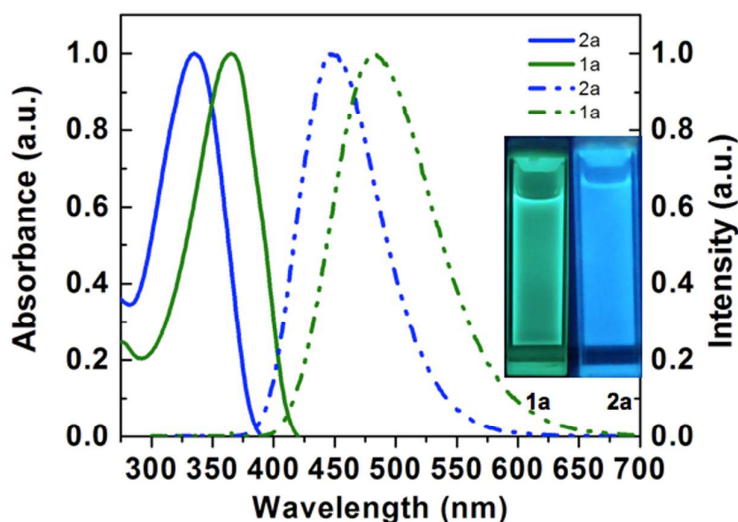


Figure 13. Normalized absorption (solid trace) and emission spectra (dotted trace) in THF solution obtained for **1a** (green trace) and **2a** (blue trace). Pictures of micromolar solutions of compounds **1a** and **2a** in THF as seen with the illumination of 365 nm UV light (inset).

Dilution of these micromolar solutions in THF did not show any variation in the absorption and emission maxima, showing that these polycatenars are not aggregating at these concentrations (SI). When the concentration is gradually increased from micromolar solution to millimolar solution absorption maximum shows a slight blue shift (Fig. 14a). The emission spectra in solution with the increase in concentrations did not show any shift in the emission maxima (Fig.14b), but showed a gradual increase in the fluorescence intensity upto certain

concentration (Fig. 14c). Further increase in concentration reduced the fluorescence intensity due to the aggregation quenching (Fig. 14d). Similar behavior was observed in the case of

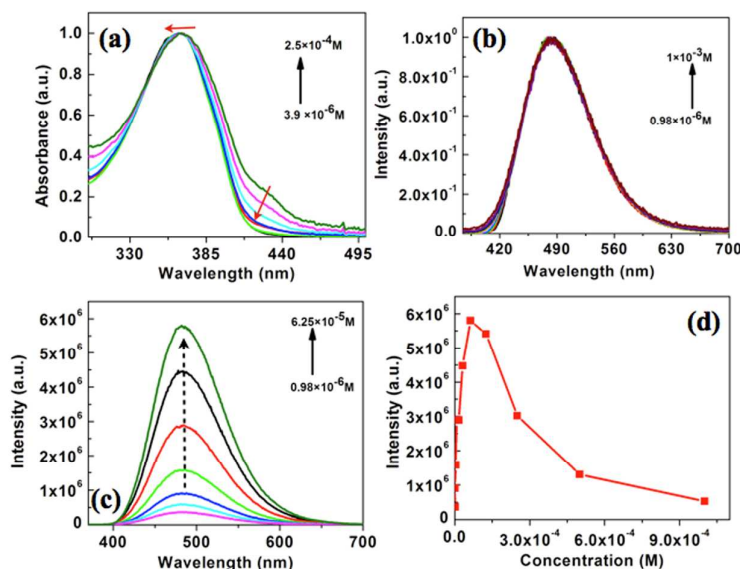


Figure 14. Normalized absorption (a) and emission (b) spectra obtained for compound **1a** as a function of concentration; Enhancement of luminescence in solution on increasing the concentration (c); A graph showing the variation of luminescence intensity with respect to concentration (d).

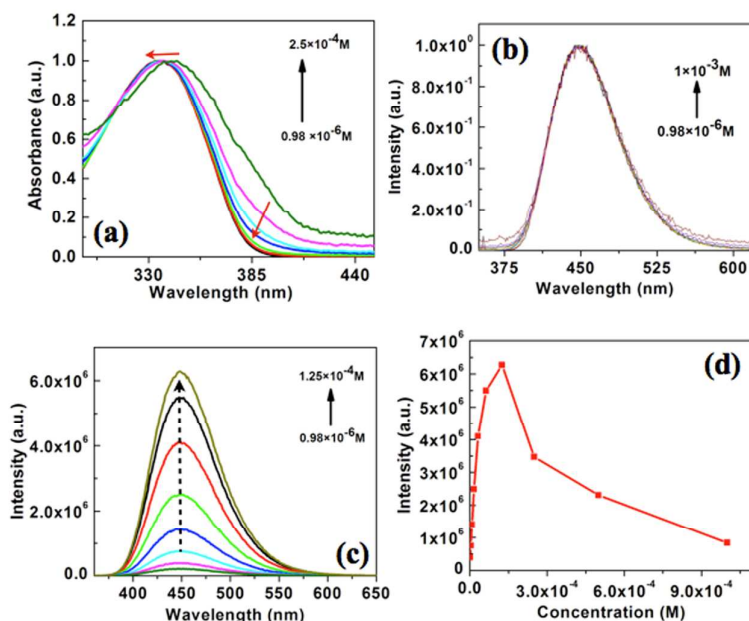


Figure 15. Normalized absorption (a) and emission (b) spectra obtained for compound **2a** as a function of concentration; Enhancement of luminescence in solution on increasing the concentration (c); A graph showing the variation of luminescence intensity with respect to concentration (d).

compound **2a** (Fig. 15). At higher concentration the absorption spectra showed a slight blue shift, while the emission spectra did not show any change. As in the case of compound **1a**, upto a certain concentration there was an increase in the intensity of fluorescence, after which there was a decrease in the intensity (Fig. 15d). This decrease may be due to the aggregation quenching. Fluorescence life-time decay profiles obtained for compounds **1a** and **2a** at concentrations corresponding to their highest fluorescence intensity exhibited a monoexponential decay with the life-time values of 1.73 and 1.44 ns respectively, confirming the presence of solvated monomers (Fig. 16).

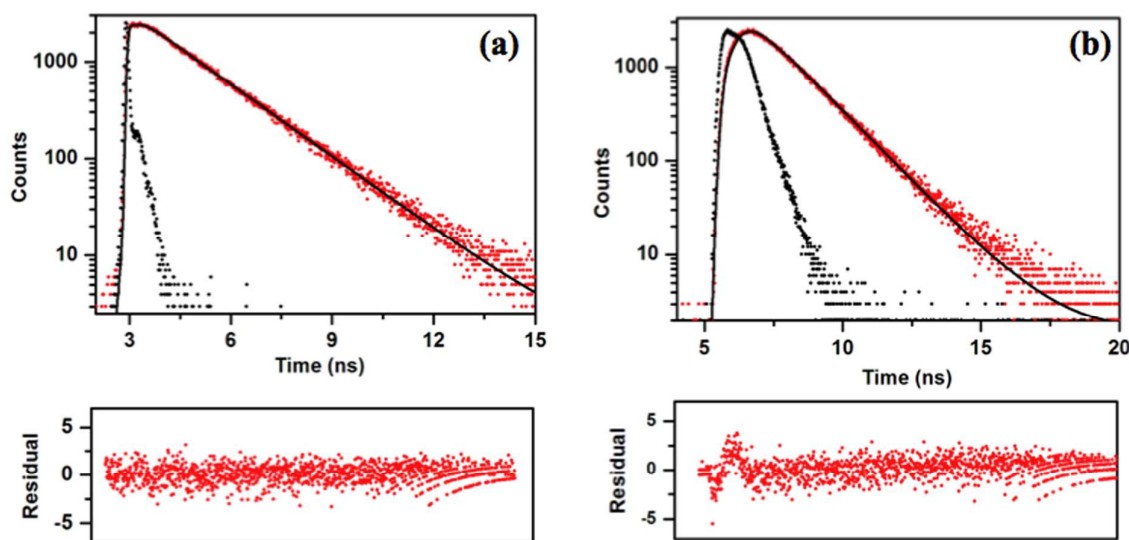


Figure 16. (a) The fluorescence decay of compound **1a** in THF ($6.25 \times 10^{-5}\text{M}$, $\lambda_{\text{exc}} = 375 \text{ nm}$) (b) fluorescence decay of compound **2a** in THF ($1.25 \times 10^{-4}\text{M}$, $\lambda_{\text{exc}} = 336 \text{ nm}$). (Red trace corresponding to the decay profile, black trace corresponding to instrument response function; the residual plot is shown below the decay plot)

We were interested to study the emissive nature of these molecules in solid state. Thin films of these molecules were prepared on glass slides by drop casting the millimolar solutions in toluene. The absorption spectra of compounds **1a** and **2a** showed structured absorption bands. Compound **1a** showed two absorption maxima centered at 301 and 385 nm, while compound **2a** also showed two absorption maxima centered at 301 and 371 nm. In comparison to their structureless solution state absorption spectra, these absorption spectra showed two absorption maxima and a blue shift. Emission spectra obtained by exciting the solutions at their absorption maxima were found to be broadened with a slight red shift. Compound **1a** showed an emission maximum centered at 485 nm, while compound **2a** showed an emission

maximum centered at 463 nm. Thus compound **1a** showed a red shift of 5 nm, while compound **2a** showed a red shift of 13 nm with respect to their solution state spectra. But under UV light of long wavelength (365 nm) these films showed similar visually perceivable emission as in the solution state for compounds **1a** and **2a** (Fig. 13 and Fig. 17b). The blue shift in the absorption bands observed for thin films in comparison to the solution state indicates that the emission is arising from the molecular aggregates, in which the molecules

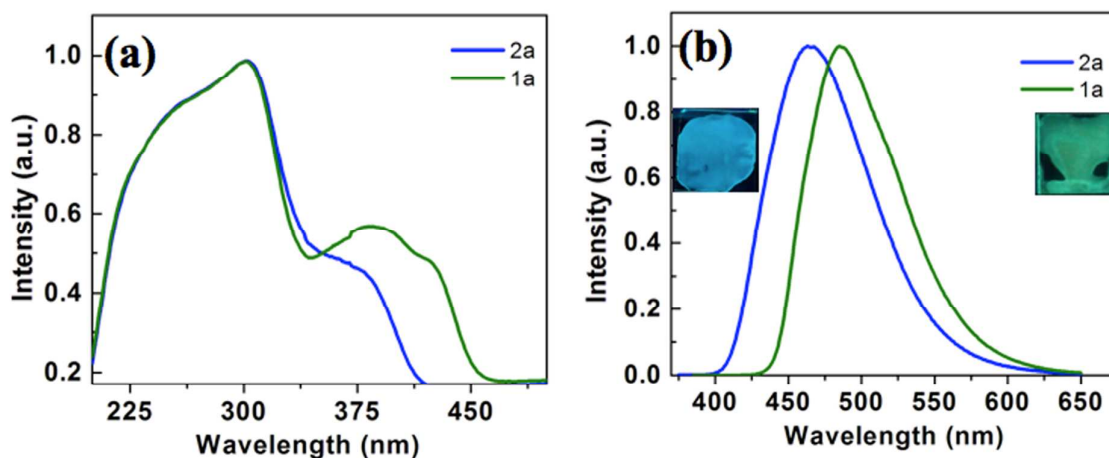


Figure 17. Normalized absorption spectra obtained for compounds **1a** (green trace) and **2a** (blue trace) in the thin film state prepared from drop casting (a); Normalized emission spectra obtained for compounds **1a** and **2a** in the thin film state (b). Inset shows the thin films of compounds **1a** and **2a** on illumination of 365 nm UV light (inset).

are stacked one above the other in a cofacial manner which is denoted as H-aggregates.⁴⁰ We have also attempted to see whether these compounds form gel in various solvents, but found that the π - π interaction between the aromatic cores alone was not sufficient for gelation. We have also prepared thin films of the sample by heating the sandwiched sample between glass slides to isotropic state. These films were suddenly cooled in their liquid crystalline state. Polarizing optical images have shown that compound **1a** was crystallized during this sudden cooling (Fig. 18c), while compound **2a** retained the texture of Col_{ob} phase (Fig. 18f). Both of the films showed good transparency (Fig. 18a and d). It is interesting to note that the thin film prepared from compound **1a** turned opaque and formed a green colored film slowly, while compound **2a** still retained the transparency and liquid crystalline texture even after 7 days (Fig. 18g). Thus it can be understood that the molecular structure of *p*-substituted polycatenars are more conducive to crystallization, while that of *m*-substituted polycatenars prevent crystallization and favors glassy state. Glassy columnar structure helps in charge migration

with the simultaneous freezing of ionic impurities, which is a favorable feature for applications in organic electronic devices.⁴¹

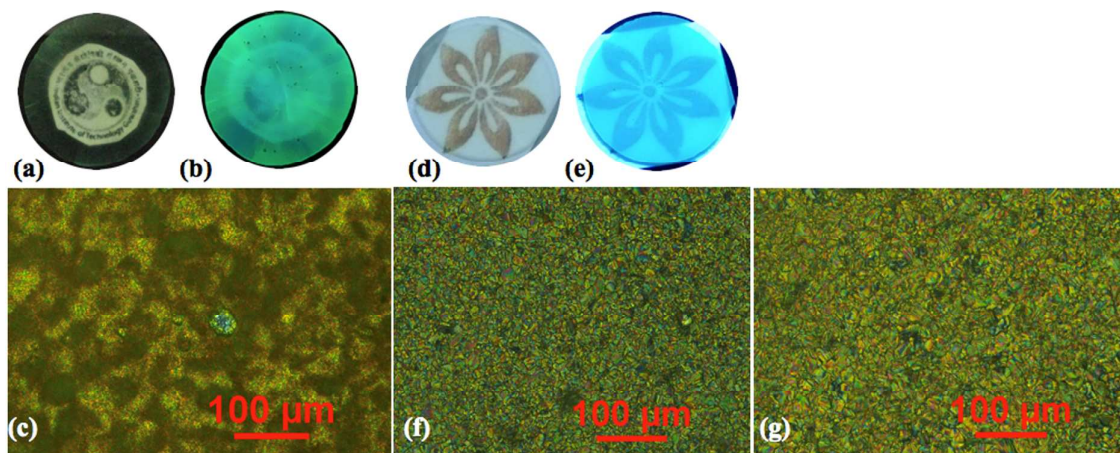


Figure 18. Thin film prepared from compound **1a** by annealing the isotropic liquid under (a) day light and (b) 365 nm UV light; POM image of the same film showing crystallization (c); Thin film prepared from compound **2a** by annealing the isotropic liquid under (d) day light and (e) 365 nm UV light; POM image of the same film showing the freezing of Col_{ob} phase (f); POM image of the film after 7 days showing the stable glassy state (g).

IV. Electrochemical properties

Energy levels of HOMO and LUMO and the band gap of the polycatenars were obtained by cyclic voltammetry (CV) and the data are tabulated in table 5. We have chosen compound **1a** and **2a** for carrying out CV studies. Both the compounds exhibited irreversible oxidation and reduction waves (See SI). The optical band gap $E_{g, opt}$ was estimated from the red edge of the absorption spectra. *p*-Substituted compounds **1a** exhibited lower band gap when compared to *m*-substituted compounds **2a-c**. Energy levels of LUMO and HOMO were determined by using the formulae $E_{LUMO} = -(4.8 - E_{1/2, Fc, Fc^+} + E_{red, onset})$ eV, $E_{HOMO} = (4.8 - E_{1/2, Fc, Fc^+} + E_{ox, onset})$ eV. *p*-Substituted compounds **1a** exhibited LUMO level -3.31 eV, and a HOMO level at -5.87 eV, while *m*-substituted compounds **2a** exhibited LUMO levels -3.29 eV, and a HOMO level at -5.98 eV. Thus the band gaps estimated from CV by using the above formula give the band gap values of -2.56 eV for compound **1a** and -2.69 eV for compound **2a** respectively. These values are slightly lesser than their respective optical band gap values (Table 4). When compared to their star shaped analogues, polycatenars exhibit

slightly lower LUMO and higher HOMO levels. As a result there is a reduction in the band gap of polycatenars when compared to their star shaped analogue^{33b} (Fig. 19).

Table 5. Electrochemical^{a,b} properties of polycatenars

Entry	$E_{\text{red}}^{\text{d}}$	$E_{\text{oxd}}^{\text{d}}$	$E_{\text{HOMO}}^{\text{c,e}}$	$E_{\text{LUMO}}^{\text{c,f}}$	$\Delta E_{\text{CV}}^{\text{c,g}}$
1a	-0.93	1.63	-5.87	-3.31	2.56
2a	-0.95	1.74	-5.98	-3.29	2.69

^amicromolar solutions in THF; ^bExperimental conditions: Ag/AgNO₃ as reference electrode, Glassy carbon working electrode, Platinum rod counter electrode, TBAP (0.1 M) as a supporting electrolyte, room temperature, scanning rate of 0.05 mVs⁻¹; ^cIn electron volts (eV), ^dIn volts (V), ^e Estimated from the onset oxidation peak values by using from the formula $E_{\text{HOMO}} = (4.8 - E_{1/2, \text{Fc/Fc}^+} + E_{\text{ox, onset}})$ eV, ^fEstimated from the onset reduction peak values by using $E_{\text{LUMO}} = -(4.8 - E_{1/2, \text{Fc/Fc}^+} + E_{\text{red, onset}})$ eV. ^gEstimated from the formula $\Delta E_{\text{CV}} = E_{\text{HOMO}} - E_{\text{LUMO}}$ eV.

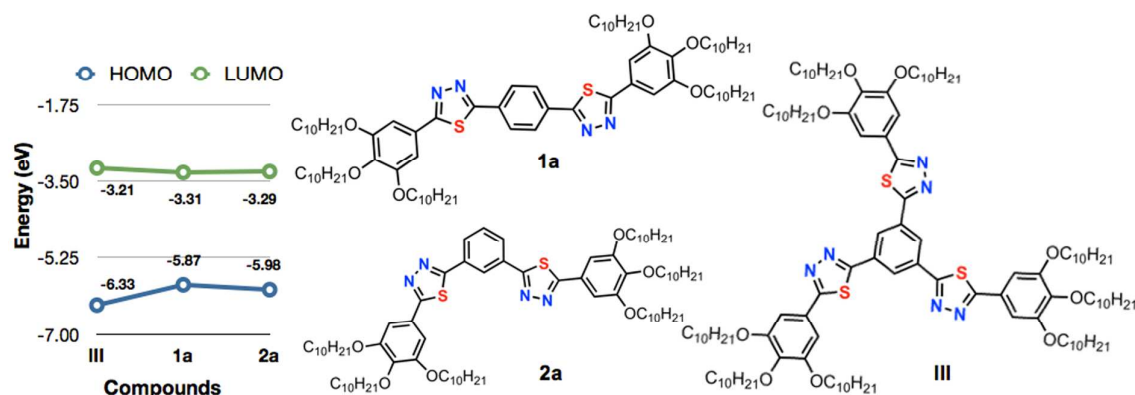


Figure 19. Comparison of frontier molecular orbitals for compounds **1a**, **2a** and **III**.

V. Experimental Section

Commercially available chemicals were used without any purification; solvents were dried following the standard procedures. Chromatography was performed using either silica gel (60-120 and 100-200) or neutral aluminium oxide. For thin layer chromatography, aluminium sheets pre-coated with silica gel were employed. IR spectra were recorded on a Perkin Elmer IR spectrometer at normal temperature by using KBr pellet. The spectral positions are given in wave number (cm⁻¹) unit. NMR spectra were recorded using Varian Mercury 400 MHz or Bruker 600 MHz NMR spectrometer (at 298K). For ¹H NMR spectra, the chemical shifts are reported in ppm relative to TMS as an internal standard. Coupling constants are given in Hz. Mass spectra were obtained from MALDI-TOF mass spectrometer in Laser Desorption positive mode using α -cyano-4-hydroxycinnamic acid matrix or from High Resolution Mass Spectrometer.

The mesogenic compounds were investigated for their liquid crystalline behavior (birefringence and fluidity) by employing a polarizing optical microscope (POM) (Nikon Eclipse LV100POL) equipped with a programmable hot stage (Mettler Toledo FP90). Clean glass slides and coverslips were employed for the polarizing optical microscopic observations. The transition temperatures and associated enthalpy changes were determined by differential scanning calorimeter (Mettler Toledo DSC1) under nitrogen atmosphere. Peak temperatures obtained in DSC corresponding to transitions were in agreement with the POM observations. The transition temperatures obtained from calorimetric measurements of the first heating and cooling cycles at a rate of 5 °C/min are tabulated. In the cases where the DSC signatures are not observed for the phase transitions, the transition temperatures have been taken from POM observations. Temperature dependent X-ray diffraction studies were carried on unaligned powder samples in Lindemann capillaries (1 mm diameter) held in programmable hot stage and irradiated with CuK α radiation ($\lambda = 1.5418 \text{ \AA}$). The samples were filled in the capillary tube in their isotropic state and their both ends were flame sealed. The apparatus essentially consisted of a PANalytical X'Pert PRO MP X-ray diffractometer consisting of a focusing elliptical mirror and a fast high resolution detector (PIXCEL). Thermogravimetric analysis (TGA) was performed using thermogravimetric analyzer (Mettler Toledo, model TG/SDTA 851e) under constant nitrogen flow at a heating rate of 10 °C/min. UV-Vis spectra were obtained by using Perkin-Elmer Lambda 750, UV/VIS/NIR spectrometer. Fluorescence emission spectra in solution state were recorded with Horiba Fluoromax-4 fluorescence spectrophotometer or Perkin Elmer LS 50B spectrometer. Cyclic Voltammetry studies were carried out using a PAR Model 700D series Electrochemical workstation. Time resolved fluorescence was measured using an Edinburgh Instruments Life Spec II instrument. Here the fluorescence lifetimes were determined by a time-correlated single photon counting method. A Hamamatsu microchannel plate (MCP) detector that has a response time of 50 ps was used in the abovementioned instrument. A picosecond 375 nm laser diode and 336 LED were used as the light sources. The full width at half maxima for the laser diode and the LED are 90 ps and 570 ps respectively. The fluorescence emission maxima for the corresponding species has been chosen as the monitoring wavelength in the time resolved fluorescence measurements. The data were analyzed using a reconvolution method using the software provided by Edinburgh instruments.

VI. Summary

In summary, we have synthesized two series of polycatenars containing 1,3,4-thiadiazole moiety in their molecular structure. The main difference between the two series is the position at which the 1,3,4-thiadiazole moiety is connected to a central benzene ring. In the first series the thiadiazole moieties are connected to the central benzene ring at 1,4 position (*p*-substituted), while in the second series the thiadiazole moiety is connected at 1,3 position (*m*-substituted) to the central benzene ring. The thermal behavior was studied with the help of POM, TGA, DSC and powder XRD studies. Both the series stabilized enantiotropic columnar phase. *p*-Substituted polycatenars stabilized Col_h and/or Col_{ob} phase, while *m*-substituted polycatenars exhibited Col_{ob} phase exclusively. *m*-substituted polycatenars showed enhanced core-core interaction in comparison to their *p*-substituted polycatenars. In both the series mesophase range is decreased with the increase in the chain length. Incorporation of sulphur in the molecular structure enhanced the thermal range of mesophase with respect to their oxadiazole counterparts. Polycatenar thiadiazoles exhibited reduced mesophase range when compared to the star shaped thiadiazole derivatives.

Both the series exhibited luminescence in solution. *p*-Substituted compounds showed green emission, while *m*-substituted compounds exhibited blue emission in solution state. Thus the substitution plays a very important role in the luminescence properties of these molecules. Most importantly, the thin films prepared by the drop casting or by annealing from the isotropic state showed similar visually perceivable emission. The length of the peripheral tails did not have much effect on the absorption and emission behavior of these compounds. Cyclic Voltammetry studies have shown that *p*-substituted polycatenars showed lower bandgap than the *m*-substituted compounds. Both the polycatenars exhibited a lower band gap than their star shaped analogue. Thus in this report we have shown that regioisomerism affects significantly on the self-assembly and photophysical behavior of 1,3,4-thiadiazole based polycatenars.

VII. Associated Content

The synthesis and characterization details, ¹H NMR, ¹³C NMR spectra of all new compounds, absorption and emission spectra, POM photographs, DSC thermograms, XRD profiles of LC compounds, TGA curves and Cyclic voltammograms are provided as electronic supporting information. This material is available free of charge via the Internet.

Acknowledgements

ASA sincerely thanks Science and Engineering Board (SERB), DST, Govt. of India and Board of Research in Nuclear Sciences-Department of Atomic Energy (BRNS-DAE) for funding this work through the project No. SB/S1/PC-37/2012 and No. 2012/34/31/BRNS/1039 respectively. We thank Ministry of Human Resource Development for Centre of Excellence in FAST (F. No. 5-7/2014-TS-VII). ASA acknowledges Central Instrumentation Facility, IIT Guwahati for analytical facilities. We acknowledge Dr. Chandan Mukherjee, IITGuwahati for providing his Electrochemical workstation.

References

1. (a) S. Chandrasekhar, in *Liquid Crystals*, 2nd ed.; Cambridge University Press: New York, 1994; (b) T. Geelhaar, K. Griesar and B. Reckmann, *Angew. Chem. Int. Ed.* 2013, **52**, 8798-8809; (c) C. Tschierske, *Angew. Chem. Int. Ed.* 2013, **52**, 8828-8878; (d) J. W. Goodby, P. J. Collings, T. Kato, C. Tschierske, H. Gleeson and P. Raynes, Eds. *Handbook of Liquid Crystals: Fundamentals*, Wiley-VCH: Weinheim, Germany, 2014; *Vol. 1*.
2. (a) D. Demus, *Liq. Cryst.* 1989, **5**, 75-110; (b) C. Tschierske, *J. Mater. Chem.* 1998, **8**, 1485-1508; (c) C. Tschierske, *J. Mater. Chem.* 2001, **11**, 2647-2671; (d) C. Tschierske, *Annu. Rep. Prog. Chem. Sect. C*, 2001, **97**, 191-267; (e) C. Tschierske, *Curr. Opin. Colloid Interface Sci.* 2002, **7**, 69-80.
3. (a) F. Reinitzer, *Monatsch. Chem.* 1888, **9**, 421-441; (b) F. Reinitzer, *Liq. Cryst.* 1989, **5**, 7-18.
4. S. Chandrasekhar, B. K. Sadashiva and K. A. Suresh, *Pramana*, 1977, **9**, 471-480.
5. (a) C. T. Imrie and G. R. Luckhurst, in *Handbook of liquid crystals, Vol-2B*, Eds.: D. Demus, J. W. Goodby, G. W. Gray and H. -W. Spiess, V. Vill, Wiley-VCH, Germany, 1998, part – III, p.799; (b) C. T. Imrie and P. A. Henderson, *Curr. Opin. Colloid Interface Sci.* 2002, **7**, 298-311; (c) C. T. Imrie in *Structure and Bonding - Liquid crystals, II*, Ed: D. M. P. Mingos, Springer-Verlag, 1999, p.149; (d) N. Tamaoki, *Adv. Mater.* 2001, **13**, 1135-1147; (e) C. V. Yelamaggad, G. Shanker, U. S. Hiremath, and S. K. Prasad, *J. Mater. Chem.* 2008, **18**, 2927-2949; (f) A. S. Achalkumar, U. S. Hiremath, D. S. Shankar Rao and C. V. Yelamaggad, *Liq. Cryst.* 2011, **38**, 1563-1589; (g) V. Borshch, Y. K. Kim, J. Xiang, M. Gao, A. Jakli, V. P. Panov, J. K. Vij, C. T. Imrie, M. G. Tamba, G. H. Mehl and O. D. Lavrentovich, *Nature Communications*, 2013, **4**, 1-8.
6. (a) T. Niori, T. Sekine, J. Watanabe, T. Furukawa and H. Takezoe, *J. Mater. Chem.* 1996, **6**, 1231-1233; (b) R. A. Reddy and C. Tschierske, *J. Mater. Chem.* 2006, **16**, 907-961; (c) H. Takezoe and Y. Takanishi, *Jpn. J. of App. Phys.* 2006, **45**, No. 2A, 597-625.

7. (a) K. Borisch, S. Diele, P. Goring, H. Muller and C. Tschierske, *Liq. Cryst.* 1997, **22**, 427-443; (b) K. Borisch, S. Diele, P. Goring, H. Kresse and C. Tschierske, *J. Mater. Chem.* 1998, **8**, 529-543; (c) F. Liu, R. Kieffer, X. Zeng, K. Pelz, M. Prehm, G. Ungar and C. Tschierske, *Nature Communications*, 2012, **3**, 1104-1107; (d) C. Tschierske, *Isr. J. Chem.* 2012, **52**, 935-959.
8. (a) H. Zeng and T. M. Swager, *J. Am. Chem. Soc.* 1994, **116**, 761-762; (b) T. M. Swager and H. Zeng, *Mol. Cryst. Liq. Cryst.* 1995, **260**, 301-306.
9. (a) A. Pegenau, P. and Tschierske, *Chem. Commun.* 1996, 2563-2564; (b) M. Lehmann, R. I. Gearba, M. H. J. Koch, and D. A. Ivanov, *Chem. Mater.* 2004, **16**, 374-376; (c) M. Lehmann and M. Jahr, *Chem. Mater.* 2008, **20**, 5453-5456; (d) H. Detert, M. Lehmann and H. Meier, *Materials*, 2010, **3**, 3218-3330; (e) M. Lehmann, *Chem. Eur. J.* 2009, **15**, 3638-3651.
10. M. Lee, D. -W. Lee and B. -K. Cho, *J. Am. Chem. Soc.* 1998, **120**, 13258-13259.
11. (a) J. H. Cameron, A. Facher, G. Lattermann and S. Diele, *Adv. Mater.* 1997, **9**, 398-403; (b) A. Pegenau, T. Hegmann, C. Tschierske and S. Diele, *Chem. Eur. J.* 1999, **5**, 1643-1660; (c) S. I. Stupp, M. Keser and G. N. Tew, *Polymer*, 1998, **39**, 4505-4508; (d) H. Meier, M. Lehmann, and U. Kolb, *Chem. Eur. J.* 2000, **6**, 2462-2469; (e) V. Percec, A. E. Dulcey, V. S. K. Balagurusamy, Y. Miura, J. Smidrkal, M. Peterca, S. Nummelin, U. Edlund, S. D. Hudson, P. A. Heiney, H. Duan, S. N. Magonov, and S. A. Vinogradov, *Nature*, 2004, **430**, 764-768; (f) M. Lehmann, C. Köhn, H. Meier, S. Renker and A. Oehlhof, *J. Mater. Chem.* 2006, **16**, 441-451; (g) B. M. Rosen, C. J. Wilson, D. A. Wilson, M. Peterca, M. R. Imam, and V. Percec, *Chem Rev.* 2009, **109**, 6275-6540; (h) B. Donnio, *Inorganica Chimica Acta*, 2014, **409**, 53-67.
12. (a) J. Malthete, A. M. Levulut and N. H. Tinh, *J. Phys. Lett.* 1985, **46**, 875-880; (b) J. Malthete, H. T. Nguyen and C. Destrade, *Liq. Cryst.* 1993, **13**, 171-187; (c) H.-T. Nguyen, C. Destrade and J. Malthete, *Adv. Mater.* 1997, **9**, 375-388; (d) K. E. Rowe and D. W. Bruce, *J. Mater. Chem.* 1998, **8**, 331-341; (e) B. P. Hoag and D. L. Gin, *Adv. Mater.* 1998, **10**, 1546-1551; (f) T. Yasuda, K. Kishimoto and T. Kato, *Chem. Commun.*, 2006, 3399-3401; (g) J. Seo, S. Kim, S. H. Gihm, C. R. Park and S. Y. Park, *J. Mater. Chem.* 2007, **17**, 5052-5057; (h) S.-J. Yoon, J. H. Kim, K. S. Kim, J. W. Chung, B. Heinrich, F. Mathevet, P. Kim, B. Donnio, A.-J. Attias, D. Kim and S. Y. Park, *Adv. Funct. Mater.* 2012, **22**, 61-69; (i) V. N. Kozhevnikov, B. Donnio and D. W. Bruce, *Angew. Chem. Int. Ed.* 2008, **47**, 6286-6289; (j) C. Alstermark, M. Eriksson, M. Nilsson, C. Destrade and H. T. Nguyen, *Liq Cryst.* 1990, **8**, 75-80; (k) D. Fazio, C. Mongin, B. Donnio, Y. Galerne D. Guillon and D.W. Bruce. *J. Mater. Chem.* 2001, **11**, 2852-2863; (l) D. M. Huck, H. L. Nguyen, P. N. Horton, M. B. Hursthouse, D. Guillon, B. Donnio and D. W. Bruce, *Polyhedron*. 2006, **25**, 307-324; (m) A. I. Smirnova and D. W. Bruce, *J. Mater. Chem.* 2006, **16**, 4299-4306; (n) E. Gorecka, D. Pocięcha, J. Mieczkowski, J. Matraszek, B. Donnio and D. Guillon, *J. Am. Chem. Soc.* 2004, **126**, 15946-15947; (o) C. Tschierske, *Angew. Chem. Int. Ed.* 2000, **39**, 2454-2458; (p) E. Gorecka, D. Pocięcha, J. Matraszek, J. Mieczkowski, Y. Shimbo, Y. Takanishi and H. Takezoe, *Phys. Rev. E.* 2006, **73**, 31704-31708; (q) J. Barbera, E. Cavero, M. Lehmann, J. L. Serrano, T. Sierra and J. T. Vazquez, *J. Am.*

- Chem. Soc.* 2003, **125**, 4527-4533; (r) D. Pucci, *Liq Cryst.* 2011, **38**, 1451-1465; (s) K. Han and B.-K. Cho, *Soft Matter*, 2014, **10**, 7588-7594.
13. J. H. Porada and D. Blunk, *J. Mater. Chem.* 2010, **20**, 2956- 2958.
14. (a) K. Mullen and G. Wegner, *Electronic Materials: The Oligomer Approach*; Wiley-VCH: Weinheim, 1998; (b) R. E. Martin and F. Diederich, *Angew. Chem. Int. Ed.* 1999, **38**, 1350-1377; (c) F. S. Precup-Bлага, J. C. Garcia-Martinez, A. P. H. J. Schenning and E. W. Meijer, *J. Am. Chem. Soc.* 2003, **125**, 12953-12960; (d) F. Lincker, P. Bourgun, P. Masson, P. Didier, L. Guidoni, J.-Y. Bigot, J.-F. Nicoud, B. Donnio, and D. Guillon, *Org. Lett.* 2005, **7**, 1505-1508; (e) M. O'Neill and S.M. Kelly, *Adv Mater.* 2003, **15**, 1135-1146; (f) A. Contoret, A. Eastwood, S. Farrar, S. M. Kelly, E Nicholls, M. O'Neill, G. Richards and C. Wu, *Mol. Cryst. Liq. Cryst.* 2001, **368**, 271-278; (g) N. H. Sultana, S.M. Kelly, B. Mansoor and M. O'Neill, *Liq Cryst.* 2007, **34**, 1307-1316; (h) C. Gadermaier, G. Lanzani, G. Cerullo, M. Zavelani-Rossi, U. Theissel, B. Hoag, G. Leising, S. De Selvestri and D. L. Gin. *Synth Met.* 2001, **121**, 1323-1324; (i) A. P. Sivadas, N. S. S. Kumar, D. D. Prabhu, S. Varghese, S. K. Prasad, D. S. S. Rao, and S. Das, *J. Am. Chem. Soc.* 2014, **136**, 5416-5423.
15. C. V. Yelamaggad, G. Shanker, R. V. R. Rao, D. S. S. Rao, S. K. Prasad, and V. V. S. Babu, *Chem. Eur. J.* 2008, **14**, 10462-10471.
16. N. G. Nagaveni, M. Gupta, A. Roy, and V. Prasad, *J. Mater. Chem.* 2010, **20**, 9089-9099.
17. V. S. K. Balagurusamy, S. K. Prasad, S. Chandrasekhar, S. Kumar, M. Manickam and C. V. Yelamaggad, *Pramana*, 1999, **53**, 3-11.
18. (a) B. A. Gregg, M. A. Fox, and A. J. Bard, *J. Phys. Chem.* 1990, **94**, 1586-1598; (b) K. Petritsch, R. H. Friend, A. Lux, G. Rozenberg, S. C. Moratti, and A. B. Holmes. *Synth. Met.* 1999, **102**, 1776- 1777; (c) L. S. Mende, A. Fechtenkotter, K. Mullen, E. Moons, R. H. Friend and J. D. MacKenzie, *Science* 2001, **293**, 1119 – 1122; (d) N. Tchebotareva, X. Yin, M. D. Watson, P. Samori, J. P. Rabe, and K. Mullen. *J. Am. Chem. Soc.* 2003, **125**, 9734-9739; (e) P. Samori, X. Yin, N. Tchebotareva, Z. Wang, T. Pakula, F. Jäckel, M. D. Watson, A. Venturini, K. Müllen, and J. P. Rabe. *J. Am. Chem. Soc.* 2004, **126**, 3567-3575; (f) Q. Sun, L. Dai, X. Zhou, L. Li and Q. Li, *Applied Physics Letters*, 2007, **91**, 253505/1-253505/3; (g) H. C. Hesse, J. Weickert, M. Al-Hussein, L. Dössel, X. Feng, K. Mullen and L. S. Mende, *Solar Energy Materials & Solar Cells*, 2010, **94**, 560-567; (h) X.-Y. Liu, T. Usui, H. Iino and J. -I. Hanna, *J. Mater. C.* 2013, **1**, 8186-8193.
19. (a) A. Bacher, I. Bleyl, C. H. Erdelen, D. Haarer, W. Paulus and H. W. Schmidt, *Adv. Mater.* 1997, **9**, 1031-1035; (b) T. Christ, B. Glusen, A. Greiner, A. Kellner, R. Sander, V. Stumpflen, V. Tsukruk, and J. H. Wendorff, *Adv. Mater.* 1997, **9**, 48-51; (c) I. H. Stapff, V. Stumpflen, J. H. Wendorff, D. B. Spohn and D. Möbius. *Liq. Cryst.* 1997, **23**, 613-617; (d) A. Bacher, C. H. Erdelen, W. Paulus, H. Ringsdorf, H. W. Schmidt and P. Schuhmacher, *Macromolecules*, 1999, **32**, 4551-4557; (e) I. Seguy, P. Destruel, and H. Bock, *Synthetic Metals*, 2000, **111**, 15-18; (f) T. Hassheider, S. A. Benning, H. S. Kitzerow, M. F. Achard and H. Bock, *Angew. Chem. Int. Ed.* 2001, **40**, 2060-2063; (g) S. Alibert-Fouet, S. Dardel, H. Bock, M. Oukachmih, S. Archambeau, I. Seguy, P. Jolinat, and P. Destruel, *ChemPhysChem*,

- 2003, **4**, 983-985; (h) C. R. McNeill and N. C. Greenham, *Adv. Mater.* 2009, **21**, 1-11; (i) M. O'Neill and S. M. Kelly, *Adv. Mater.* 2011, **23**, 566-584; (j) J. Eccher, G. C. Faria, H. Bock, H. von Seggern and I. H. Bechtold, *ACS Appl Mater Interfaces*, 2013, **5**, 11935-11943.
20. (a) P. R. L. Malenfant, C. D. Dimitrakopoulos, J. D. Gelorme, L. L. Kosbar, T. O. Graham, A. Curioni and W. Andreoni, *Appl. Phys. Lett.* 2002, **80**, 2517; (b) A. M. van de Craats, N. Stutzmann, O. Bunk, M. M. Nielsen, M. Watson, K. Mullen, H. D. Chanzy, H. Sirringhaus and R. H. Friend, *Adv. Mater.* 2003, **15**, 495-499; (c) S. Cherian, C. Donley, D. Mathine, L. LaRussa, W. Xia and N. Armstrong, *J. Appl. Phys.* 2004, **96**, 5638-5643; (d) R. J. Chesterfield, J. C. McKeen, C. R. Newman, P. C. Ewbank, D. A. da Silva Filho, J. L. Bredas, L. L. Miller, K. R. Mann, and C. D. Frisbie, *J. Phys. Chem. B.* 2004, **108**, 19281-19292; (e) I. O. Shklyarevskiy, P. Jonkheijm, N. Stutzmann, D. Wasserberg, H. J. Wondergem, P. C. M. Christianen, A. P. H. J. Schenning, D. M. de Leeuw, Z. Tomovic, J. Wu, K. Mullen and J. C. Maan, *J. Am. Chem. Soc.* 2005, **127**, 16233-16237; (f) W. Pisula, A. Menon, M. Stepputat, I. Lieberwirth, U. Kolb, A. Tracz, H. Sirringhaus, T. Pakula and K. Mullen, *Adv. Mater.* 2005, **17**, 684-689. (g) S. Xiao, M. Myers, Q. Miao, S. Sanaur, K. Pang, M. L. Steigerwald and C. Nuckolls, *Angew. Chem. Int. Ed.* 2005, **44**, 7390-7394; (h) H. Sirringhaus, *Adv. Mater.* 2005, **17**, 2411-2425; (i) J. Y. Cho, B. Domercq, S. C. Jones, J. Yu, X. Zhang, Z. An, M. Bishop, S. Barlow, S. R. and J. Kippelen, *J. Mater. Chem.* 2007, **17**, 2642-2647. (j) Y. Shimizu, K. Oikawa, K. Nakayama, and D. Guillon, *J. Mater. Chem.* 2007, **17**, 4223-4229; (k) H. N. Tsao, H. J. Rader, W. Pisula, A. Rouhanipour and K. Mullen, *Phys. Stat. Sol. A.* 2008, **205**, 421-429; (l) H. N. Tsao, W. Pisula, Z. Liu, W. Osikowicz, W. R. Salaneck, and K. Mullen, *Adv. Mater.* 2008, **20**, 2715-2719; (m) R. Schmidt, J. H. Oh, Y. S. Sun, M. Deppisch, A. M. Krause, K. Radacki, H. Braunschweig, M. Konemann, P. Erk, Z. Bao and F. Wurthner, *J. Am. Chem. Soc.* 2009, **131**, 6215-6228; (n) J. P. Bramble, D. J. Tate, D. J. Revill, K. H. Sheikh, J. R. Henderson, F. Liu, X. Zeng, G. Ungar, R. J. Bushby and S. D. Evans, *Adv. Funct. Mater.* 2010, **20**, 914-920; (o) J. Cattle, P. Bao, J. P. Bramble, R. J. Bushby, S. D. Evans, J. E. Lydon and D. J. Tate, *Adv. Funct. Mater.* 2013, **23**, 5997-6006.
21. (a) J. D. Wright, P. Roisin, G. P. Rigby, R. J. M. Nolte, M. J. Cook and S. C. Thorpe, *Sens. Actuators B.* 1993, **13**, 276-280; (b) J. Clements, N. Boden, T. D. Gibson, R. C. Chandler, J. N. Hulbert and E. A. Ruck-Keene, *Sens. Actuators B.* 1998, **47**, 37-42; (c) N. Boden, R. J. Bushby, J. Clements and B. Movaghar, *J. Mater. Chem.* 1999, **9**, 2081-2086; (d) V. Bhalla, A. Gupta, M. Kumar, D. S. S. and K. Prasad, *ACS Appl Mater Interfaces*, 2013, **5**, 672-679.
22. (a) D. D. L. Chung, *J. Mater. Sci.* 2002, **37**, 1475-1489; (b) A. and Venkateswara Rao, *Mater. Manufact. Processes*, 2004, **19**, 177-186; (c) K. Kawata and O. Nobuyosi, *Fujifilm Res. Dev.* 2006, **51**, 80-85.
23. (a) A. Seed, *Chem. Soc. Rev.* 2007, **36**, 2046-2069; (b) B. Roy, N. De and K. C. Majumdar, *Chem. Eur. J.* 2012, **18**, 14560-14588; (c) J. Han, *J. Mater. Chem. C.* 2013, **1**, 7779-7797; (d) R. K. Gupta, S. K. Pathak, B. Pradhan, D. S. Shankar Rao, S. Krishna Prasad and A. S. Achalkumar, *Soft Matter*, 2015, **11**, 3629-3636.

24. A. C. Grimsdale, K. Leok Chan, R. E. Martin, P. G. Jokisz and A. B. Holmes, *Chem Rev.* 2009, **109**, 897-1091.
25. (a) C. S. Wang, G. Y. Jung, Y. L. Hua, C. Pearson, M. R. Bryce, M. C. Petty, A. S. Batsanov, A. E. Goeta and J. A. K. Howard, *Chem. Mater.* 2001, **13**, 1167-1173; (b) A. P. Kulkarni, C. J. Tonzola, A. Babel and S.A. Jenekhe, *Chem. Mater.* 2004, **16**, 4556-4573;
26. J. Han, X. Y. Chang, L. R. Zhu, M.-L. Pang, J. B. Meng, S. S.-Y. Chui, S. W. Lai and V. A. L. Roy, *Chem. Asian J.* 2009, **4**, 1099-1107.
27. Y. Hu, C.-Y. Li, X.-M. Wang, Y.-H. Yang and H.-L. Zhu, *Chem Rev.* 2014, **114**, 5572-5610.
28. (a) M. Parra, S. Hernandez, J. Alderete and C. Zuniga, *Liq. Cryst.* 2000, **27**, 8, 995-1000; (b) A. A. Kiryanov, P. Sampson and A. J. Seed, *J. Org. Chem.* 2001, **66**, 7925-7929; (c) M. W. Schroder, S. Diele, G. Pelzl, N. Pancenko and W. Weissflog, *Liq. Cryst.* 2002, **29**, 1039-1046; (d) M. Parra, J. Alderete and C. Zuniga, *Liq. Cryst.* 2004, **31**, 1531-1537; (e) T. Hegmann, B. Neumann, R. Wolf and C. Tschierske, *J. Mater. Chem.* 2005, **15**, 1025-1034; (f) M. Parra, J. Vergara, P. Hidalgo, J. Barbera and T. Sierra, *Liq. Cryst.* 2006, **33**, 739-745; (g) B. Sybo, P. Bradley, A. Grubb, S. Miller, K. J. W. Proctor, L. Clowes, M. R. Lawrie, P. Sampson and A. J. Seed, *J. Mater. Chem.* 2007, **17**, 3406-3411; (h) C. F. He, G. J. Richards, S. M. Kelly, A. E. A. Contoret and M. O. Neill, *Liq. Cryst.* 2007, **34**, 1249-1267; (i) J. Han, X. Y. Chang, L. R. Zhu, Y. M. Wang, J. B. Meng, S.W. Lai and S. S.-Y. Chui, *Liq. Cryst.* 2008, **35**, 1379-1394; (j) J. H. Tomma, I. H. Rou'íl and A. H. Al-Dujaili, *Mol. Cryst. Liq. Cryst.* 2009, **501**, 3-19; (k) M. C. McCairn, T. Kreouzis and M. L. Turner, *J. Mater. Chem.* 2010, **20**, 1999-2006; (l) A. K. Prajapati and V. Modi, *Liq. Cryst.* 2011, **38**, 191-199; (m) Q. Song, D. Nonnenmacher, F. Giesselmann and R. P. Lemieux, *J. Mater. Chem. C*, 2013, **1**, 343-350; (n) P. Tuzimoto, D. M. P. O. Santos, T. D. S. Moreira, R. Cristiano, I. H. Bechtold and H. Gallardo, *Liq. Cryst.* 2014, **41**, 1097-1108; (o) R. C. Tandel and N. K. Patel, *Liq. Cryst.* 2014, **41**, 495-502.
29. (a) M. Lehmann, J. Seltmann, A. A. Auer, E. Prochnow and U. Benedikt, *J. Mater. Chem.* 2009, **19**, 1978-1988; (b) M. Lehmann and J. Seltmann, *Beilstein J. Org. Chem.* 2009, **5**, 73 (1-9).
30. M. L. Parra, E. Y. Elgueta, J. A. Ulloa, J. M. Vergara and A. I. Sanchez, *Liq. Cryst.* 2012, **39**, 917-925.
31. (a) M. Sato, *Macromol. Rapid Commun.* 1999, **20**, 77-80; (b) M. Sato and Y. Uemoto, *Macromol. Rapid Commun.* 2000, **21**, 1220-1225; (c) M. Sato, M. Notsu, S. Nakashima and Y. Uemoto, *Macromol. Rapid Commun.* 2001, **22**, 681-686; (d) M. Sato, M. Mizoi and Y. Uemoto, *Macromol. Chem. Phys.* 2001, **202**, 3634-3641; (e) M. Sato, S. Nakashima and Y. Uemoto, *J. Polym. Sci. A Polym. Chem.* 2003, **41**, 2676-2687; (f) N. S. Al-Muaiikel, *Polym Int*, 2004, **53**, 301-306; (g) M. Sato, Y. Tada, S. Nakashima, K.-I. Ishikura, M. Handa and K. Kasuga, *J. Polym. Sci. A Polym. Chem.*, 2005, **43**, 1511-1525; (h) M. Sato, Y. Matsuoka and I. Yamaguchi, *Liq. Cryst.* 2012, **39**, 1071-1081.
32. (a) M. Parra, S. Villouta, V. Vera, J. Belmar, C. Zuniga and H. Zunza, *Naturforsch. B*, 1997, **52**, 1533-1538; (b) M. Sato, R. Ishii, S. Nakashima, K. Yonetake and J. Kido,

- Liq. Cryst.* 2001, **28**, 1211-1214; (c) C. F. He, G. J. Richards, S. M. Kelly, A. E. A. Contoret and M. O'Neill, *Liq. Cryst.* 2007, **34**, 1249-1267; (d) J. H. Tomma, I. H. Rou'il and A. H. Al-Dujaili, *Mol. Cryst. Liq. Cryst.* 2009, **501**, 3-19.
33. (a) M. K. S. Al-Malki, A. S. Hameed and A. H. Al-Dujaili, *Mol. Cryst. Liq. Cryst.* 2014, **593**, 34-42; (b) S. K. Pathak, R. K. Gupta, S. Nath, D. S. Shankar Rao, S. K. Prasad and A. S. Achalkumar, *J. Mater. Chem. C* 2015, **3**, 2940-2952.
34. (a) J. Tang, R. Huang, H. Gao, X. Cheng, M. Prehm, and C. Tschierske, *RSC Adv.* 2012, **2**, 2842-2847; (b) X. Yang, H. Dai, Q. He, J. Tang, X. Cheng, M. Prehm, and C. Tschierske, *Liq. Cryst.* 2013, **40**, 8, 1028-1034.
35. (a) A. S. Achalkumar, U. S. Hiremath, D. S. Shankar Rao, S. Krishna Prasad and C. V. Yelamaggad, *J. Org. Chem.* 2013, **78**, 527-544. (b) I. Thomsen, K. Clausen, S. Scheibye and S.-O. Lawesson, *Organic Syntheses*, 1990, **7**, 372-373.
36. S. Laschat, A. Baro, N. Steinke, F. Giesselmann, C. Hägele, G. Scalia, R. Judele, E. Kapatsina, S. Sauer, A. Schreivogel, and M. Tosoni, *Angew. Chem. Int. Ed.*, 2007, **46**, 4832-4887.
37. C. V. Yelamaggad, A. S. Achalkumar, D. S. Shankar Rao, and S. Krishna Prasad, *J. Org. Chem.* 2007, **72**, 8308-8318.
38. (a) H. Zheng, C. K. Lai and T. M. Swager, *Chem. Mater.* 1995, **7**, 2067-2077. (b) C. Destrade, P. Foucher, H. Gesparoux, H. T. Nguyen, A. M. and Malthete, *Mol. Cryst. Liq. Cryst.* 1984, **106**, 121 - 146. (c) F. Morale, R. W. Date, D. Guillon, D. W. Bruce, R. L. Finn, C. Wilson, A. J. Blake, M. Schröder and B. Donnio, *Chem. Eur. J.* 2003, **9**, 2484 - 2501. (d) C. K. Lai, C. -H. Tsai and Y.-S. Pang, *J. Mater. Chem.* 1998, **8**, 1355- 1360. (e) S. Chandrasekhar, *Adv. Liq. Cryst.* 1982, **5**, 47 - 48.
39. A. Patra and M. Bendikov, *J. Mater. Chem.*, 2010, **20**, 422-433,
40. (a) D. D. Prabhu, N. S. S. Kumar, A. P. Sivadas, S. Varghese, and S. Das, *J. Phys. Chem. B*, 2012, **116**, 13071-13080. (b) M. Kasha, H. R. Rawls and M. A. El-Bayoumi, *Pure Appl. Chem.* 1965, **11**, 371. (c) F. C. Spano, *Acc. Chem. Res.*, 2010, **43**, 429-439.
41. V. Percec, M. Glodde, T. K. Bera, Y. Miura, I. Shiyanovskaya, K. D. Singer, V. S. K. Balagurusamy, P. A. Heiney, I. Schnell, A. Rapp, H.-W. Spiess, S. D. Hudson, H. Duank, *Nature* 2002, **419**, 384-387.